

Review

Land Cover Mapping in Northern High Latitude Permafrost Regions with Satellite Data: Achievements and Remaining Challenges

Annett Bartsch ^{1,*}, Angelika Höfler ¹, Christine Kroisleitner ¹ and Anna Maria Trofaier ^{2,†}

¹ Zentralanstalt für Meteorologie und Geodynamik, Hohe Warte 38, A-1190 Vienna, Austria; angelika.hoefler@zamg.ac.at (A.H.); christine.kroisleitner@zamg.ac.at (C.K.)

² European Space Agency, Climate Office, ECSAT, Harwell Campus, Didcot OX11 0FD, Oxfordshire, UK

* Correspondence: annett.bartsch@zamg.ac.at; Tel.: +43-1-36026-2290

† Current address: The University Centre in Svalbard, P.O. Box 156, 9171 Longyearbyen, Norway; annamaria.trofaier@unis.no.

Academic Editors: Parth Sarathi Roy and Prasad S. Thenkabail

Received: 25 September 2016; Accepted: 18 November 2016; Published: 26 November 2016

Abstract: Most applications of land cover maps that have been derived from satellite data over the Arctic require higher thematic detail than available in current global maps. A range of application studies has been reviewed, including up-scaling of carbon fluxes and pools, permafrost feature mapping and transition monitoring. Early land cover mapping studies were driven by the demand to characterize wildlife habitats. Later, in the 1990s, up-scaling of in situ measurements became central to the discipline of land cover mapping on local to regional scales at several sites across the Arctic. This includes the Kuparuk basin in Alaska, the Usa basin and the Lena Delta in Russia. All of these multi-purpose land cover maps have been derived from Landsat data. High resolution maps (from optical satellite data) serve frequently as input for the characterization of periglacial features and also flux tower footprints in recent studies. The most used map to address circumpolar issues is the CAVM (Circum Arctic Vegetation Map) based on AVHRR (1 km) and has been manually derived. It provides the required thematic detail for many applications, but is confined to areas north of the treeline, and it is limited in spatial detail. A higher spatial resolution circumpolar land cover map with sufficient thematic content would be beneficial for a range of applications. Such a land cover classification should be compatible with existing global maps and applicable for multiple purposes. The thematic content of existing global maps has been assessed by comparison to the CAVM and regional maps. None of the maps provides the required thematic detail. Spatial resolution has been compared to used classes for local to regional applications. The required thematic detail increases with spatial resolution since coarser datasets are usually applied over larger areas covering more relevant landscape units. This is especially of concern when the entire Arctic is addressed. A spatial resolution around 30 m has been shown to be suitable for a range of applications. This implies that the current Landsat-8, as well as Sentinel-2 missions would be adequate as input data. Recent studies have exemplified the value of Synthetic Aperture Radar (SAR) in tundra regions. SAR missions may be therefore of added value for large-scale high latitude land cover mapping.

Keywords: classification; tundra; land cover; optical; radar

1. Introduction

Land cover information is of high value for applications in the Arctic. More than 65% of land area north of 60 degrees latitude is underlain by permanently frozen ground. Information on surface properties serves as an indicator or modeling input for the extraction of permafrost properties [1]. This also applies to assessments of carbon stores and fluxes. Permafrost is expected to change

with climate change in the upcoming decades [2]. It has been pointed out by a range of studies (e.g., Westermann et al. [1] and Otte et al. [3]) that there is a need for accurate land cover description in the northern high latitudes. A suitable circumpolar map does not yet exist to date, although a range of studies demonstrated the suitability of satellite data for this purpose on local and regional scales.

A first review on traditional Arctic land cover maps as a baseline for the development of a circumpolar map was already published in 1995 by Walker et al. [4]. The Circum-Arctic Vegetation Map (CAVM) has in the following been developed using satellite data (Advanced Very High Resolution Radiometer (AVHRR)) and published [5]. This map represents vegetation communities and is to date the only consistent map across the Arctic with the necessary detail for many applications. It is limited to the area north of the treeline and has a 1-km spatial resolution. This is insufficient for a range of applications, as this cannot capture the heterogeneous nature of Arctic land cover (e.g., [6,7]). Recent globally-available land cover maps offer higher spatial detail (300–500 m), but low thematic content.

A new land cover classification should be compatible with global maps and applicable for varying purposes. Local, regional and globally-developed datasets need to be reviewed and discussed in this context.

This paper presents the techniques used for local to regional, as well as national-scale land cover mapping and discusses their varying applications in the Arctic. This includes the use of classifications for soil carbon and carbon flux upscaling, permafrost features, as well as transition monitoring. To illustrate the need for consistent and higher thematic detail in land cover products, we have compared the classes of currently available global land cover maps to the CAVM, a widely-accepted map for coarse resolution land cover assessment [8]. The purpose of this paper is to identify the required thematic detail in high latitude permafrost regions and suitable data sources, as well as to establish related problems in current global maps and potential methods to solve them.

2. Development of Techniques for Local- to Regional-Scale Mapping

The development of retrieval methods and applications has evolved with the increasing availability of satellite data. The vast majority of land cover mapping studies utilize optical satellite data. Of high importance was the launch of the Landsat series. A number of studies on habitat mapping in Alaska and the Canadian Arctic were undertaken in the 1970s and 1980s [9]. This was extended in the early 1990s with SPOT MSS (Satellite Pour l'Observation de la Terre Multispectral Scanner System) [10] and SPOT HRV (High Resolution Visible) [9,11]. These early studies aimed specifically at habitat assessments, including water fowls, muskox and the impact of reindeer grazing. Synthetic Aperture Radar (SAR) data became available with the launch of the European ERS-1 (C-band, 5.6 cm) in 1991 and the Japanese JERS-1 (L-band, 23.5 cm) in 1992. The Russian Almaz SAR mission (S-band, 9.6 cm) operated for 17 months from 1991–1992. Shortly afterwards, studies emerged analyzing the relative information content of the data from classification algorithms applied to Almaz, ERS-1, JERS-1 and Landsat-TM (Thematic Mapper) [12] to discriminate wet tundra habitats. SAR properties alone have also been evaluated for tundra habitat classifications [13]. The efficiency of SAR data in discriminating traditional classes in geobotanical maps was shown to be lower compared to optical [12]. In 1995, Belchansky et al. [13] demonstrated that multi-look processing of the SAR data was favorable for land cover studies. Such pre-processing steps are to date standard for SAR-based land cover applications. The additional bands available with Landsat TM compared to MSS were shown to be of high value for classifications in the context of wild live studies [14]. This spectral resolution is available from most optical high to medium resolution spaceborne sensors to date [15].

Many of these early studies focused on the Alaskan North Slope ([10,12–14], 1994–1996). SPOT related studies were published for the Canadian High Arctic [9] and Scandinavia [11]. Beyond that, Mosbech and Hansen [16] compared satellite imagery and infrared aerial photography for vegetation mapping methods in East Greenland using both SPOT and Landsat TM data. They highlighted the inadequacy of satellite data to capture the fine-scaled tundra Arctic vegetation mosaic. This problem has been partially overcome to date with high spatial resolution satellites, but

remains a challenge when mapping larger areas. The heterogeneity in these landscapes has been also addressed for a study site on Svalbard by Brossard and Joly [17]. Landscape types have been retrieved from Landsat. Vegetation probabilities have been assigned to these classes rather than specific class names. This approach provides a better representation, but is until now not commonly applied.

Although AVHRR images have been available since 1978, they were not studied until the late 1990s, when the data were first analyzed for Arctic land cover assessments. Due to its coarse spatial resolution (1 km), the sensor had not been of interest, as most research at that time had a local to regional focus only. A method for mapping land cover in Canada was however developed by Cihlar et al. [18] and published in 1996. An AVHRR-based land cover map for the Alaskan North Slope was published in 1997 [19]. This was soon followed by a prototype for a circumpolar map [20]. The thematic application areas of satellite data widened at the same time. The retrieval of biogeophysical parameters, such as Net and Gross Primary Production (NPP/GPP) [21,22], came into focus. Vegetation productivity can be directly linked to the reflectance in the visible and near-infrared part of the electromagnetic spectrum. NPP and GPP are determined using multiple sources, not only from satellite-derived products alone. Liu et al. [21] demonstrated the application potential for such studies using the AVHRR land cover map of Cihlar et al. [18] for a study site in Canada in 1999.

Takeuchi et al. [23] investigated in 2003 the potential of AVHRR for up-scaling of methane emissions in the West Siberian Lowlands, which are mostly located in the boreal biome, but of interest to high latitude studies, as the boreal biome is partially underlain by permafrost. SPOT HRV data from a case study area were used to develop an approach for the retrieval of land cover fractions within the AVHRR pixels, including the classes birch forest, conifer forest, forested bog and open bog. AVHRR land cover fraction maps were subsequently used to upscale methane emissions over the entire West Siberian Lowland area.

Landsat-based classifications and their applications are well established, and methods that combine them with high spatial resolution satellite data have been frequently applied (e.g., [7,24–26]). Specific methods are required to deal with the information content in the high spatial resolution images. Moody et al. [27] presented a technical solution for unsupervised classification of land cover in multispectral satellite imagery from WorldView-2, using so-called sparse representations in learned dictionaries for Barrow on the Alaskan North Slope. This approach also considers texture information. The resulting classes seem to detect real variability, but re-grouping based on expert knowledge is suggested (e.g., vegetative versus hydrologic studies). An approach for a hybrid map (pixel-, as well as object-based classification) for up-scaling soil organic carbon using Landsat-5 TM and WorldView-2 has recently been suggested by Broderick et al. [26]. Fraser et al. [28] demonstrate that predictive ecosystem mapping can be improved with a supervised classification of SPOT HRV that uses a 28-class ecosystem map based on air-photos as training data. A number of studies have recently been published that make use of SAR data only, but utilize the different polarizations, which are acquired by modern SAR systems. Atwood et al. [29] investigated the impact of radiometric correction on the accuracy of polarimetric land cover classification with ALOS PALSAR data in 2012. This led to significant qualitative and quantitative improvements. Banks et al. [30] assessed the potential of dual polarimetric TerraSAR-X and quad-pol Radarsat-2 imagery for land cover mapping using backscatter coefficients and Kennaugh matrix elements. A combination of both sensors is suggested for the best results. The impact of the incidence angle on the scattering behavior of quad-pol Radarsat-2 data has in addition been evaluated and assessed for its potential for unsupervised classification using three polarimetric SAR classifiers [31]. Shallow incidence angle images provided better results than steep angle images. A combination of polarimetric SAR data with optical data also led to better results than using SAR data alone [32]. Duguay et al. [33] confirm the potential of polarimetric SAR for shrub mapping using the support vector machine method.

The land cover class ‘water’ has received comparably great attention at high latitudes [34] as it supports the identification of thaw lakes, which are associated with permafrost features. Both, optical and SAR data are commonly used for this purpose. Spatial resolution has been identified as crucial for their mapping [6,35], but their extent is highly variable in time. Mapping Arctic water bodies therefore demands SAR methods, as the sensor’s cloud independence ensures better sampling [36,37]. This issue is discussed in more detail in Section 4.

3. Maps for Upscaling Studies

3.1. Super-Sites

A number of sites across the Arctic developed into super-sites for satellite-derived land cover-based applications. Maps have been developed that served as input for applications, such as upscaling of soil properties and fluxes. This includes the Kuparuk basin on the Alaskan North Slope, the Usa basin in northeastern European Russia and the Lena Delta in northeastern Russia. All of these multi-purpose maps rely on Landsat MSS and/or TM data. Their location is shown in Figure 1, and their properties are summarized in Table 1.

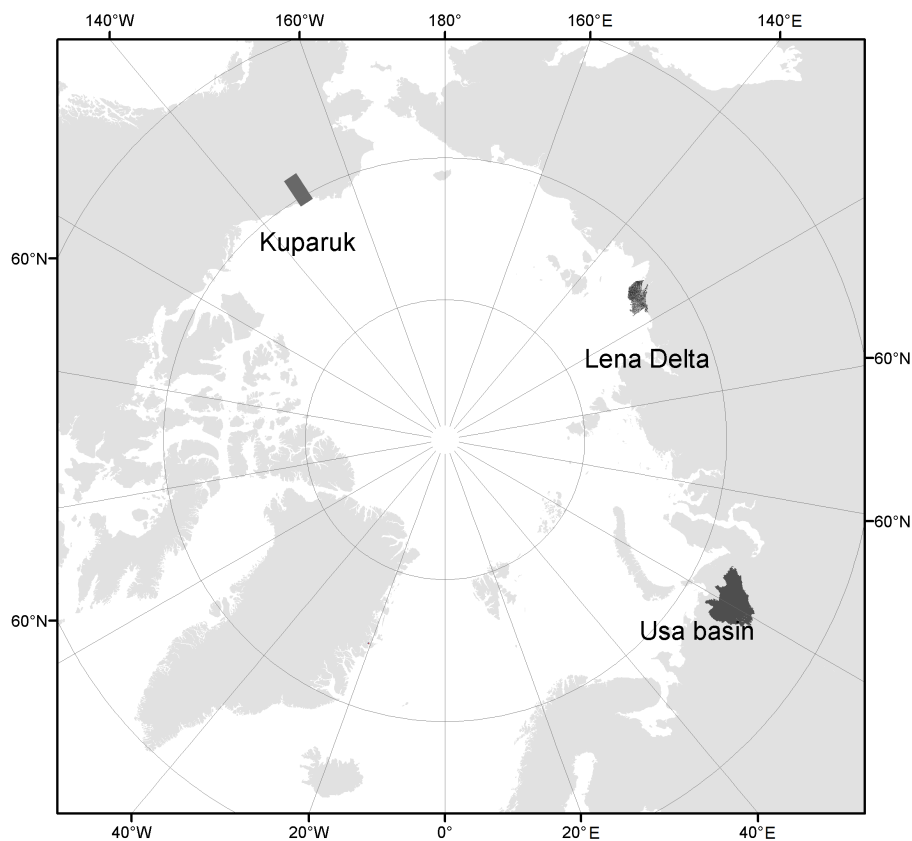


Figure 1. Location of the discussed sites with multi-purpose land cover maps from Landsat data. More details are provided in Table 1.

Table 1. Non-water classes of selected multi-purpose land cover classifications based on Landsat. The dominating land cover class is underlined. For the location, see Figure 1.

Site Name	Usa Basin (Non-Forest Part)	Kuparuk Basin	Lena Delta
Pixel size	30 m	resampled from 80 down to 50 m	30 m
Year of input data	1988/1995 (six images)	1976–1985	2000/2001 (two images)
Total area	49,370 km ²	25,300 km ²	66,470 km ²
Classification Method	semi-supervised classification of the spectrally-matched image mosaic (TM Bands 2–5, 7) (parallelepiped decision rule and maximum likelihood)	unsupervised ISODATA classification (MSS green, red and infrared bands)	unsupervised ISODATA classification (cloud masking) and supervised minimum distance classification (TM Bands 2–5, 7)
Sources	Virtanen et al. [38]	Muller et al. [39]	Schneider et al. [40]
Non-vegetated/Barrens	Mainly bare land Human infrastructures	Barren	Non-vegetated
Shrub/Trees	Willow stands Dwarf birch heath <u>Dwarf shrub moss tundra heath</u> Dry dwarf shrub, lichen tundra	Moist dwarf shrub, Tussock-graminoid tundra Moist graminoid, prostrate shrub and other shrublands	Moist to dry dwarf shrub-dominated tundra Dry moss-, sedge- and dwarf shrub-dominated tundra
Tundra/Other	Tundra with some bare peat Sparse alpine tundra Human-impacted tundra	Dry prostrate shrub tundra <u>Moist graminoid, prostrate shrub tundra</u> Wet graminoid tundra	<u>Wet sedge- and moss-dominated tundra</u> Moist grass- and moss-dominated tundra Dry grass-dominated tundra Dry tussock tundra

Initial developments have been part of a set of studies with a focus on the Kuparuk River Basin. The applicability of satellite data products (mostly Landsat based) for carbon cycle studies [22,41,42] and subsurface thermal properties ([43], Active Layer Thickness (ALT) over permafrost) was investigated. A multi-purpose land cover map has eventually been developed using Landsat MSS data in 1997 [39,44]. It was based on an unsupervised (ISODATA) classification method using the green, red and near-infrared bands. Twenty classes have been eventually distinguished, which have been interpreted for methane flux up-scaling (see Table 1). Tundra is largely distinguished by periglacial features and terrain units within them. The twenty classes are usually grouped into six units [45]. The dominating group is ‘moist graminoid, prostrate shrub Tundra’ [46]. SPOT and AVHRR NDVI (Normalized Difference Vegetation Index) values have also been investigated with respect to a potential application estimating carbon dioxide fluxes [41]. The approach used to generate the maps was subsequently transferred to the entirety of Northern Alaska [46] and compared to the AVHRR product by Walker [20], but only a 55.4% agreement was determined. Most affected are wetland/moist tundra classes and shrublands. Probable reasons are the difference in spatial resolution and the respective acquisition time. The spatial detail of wetlands and moist tundra in wetland complexes cannot be sufficiently captured by AVHRR. The acquisition time of the satellite datasets also differed with respect to the phenological stage, which has important implications for the sensor’s capabilities to identify shrublands.

The majority of methane flux up-scaling investigations in the high latitudes started only several years later, although Reeburgh et al. [41] demonstrated the capability of land cover data in tundra

areas already in 1998. Schneider et al. [40] used Landsat 7 ETM+ for up-scaling of methane emissions over the Lena Delta in 2009 (see Table 1). Classification was carried out in two steps using the unsupervised ISODATA method and supervised maximum-likelihood methods. Only the land cover class wet sedge- and moss-dominated tundra was eventually used due to its abundance in the area and importance regarding emissions. To estimate soil organic carbon and nitrogen stocks in the Lena Delta, Zubrzycki et al. [47] grouped the land cover classes to differentiate between the Holocene river terrace and the active floodplains. A Landsat-based map was also recently developed for the West Siberian Lowlands, suggesting its potential use for up-scaling of methane emissions [48].

A multi-purpose land cover classification based on Landsat TM5 has also been derived for the Usa basin in northeastern European Russia [38] using a semi-supervised approach and a similar classification scheme as for the Kuparuk basin in Alaska. The Usa basin does however also extend into the boreal biome. In total, 21 classes were therefore considered, including nine non-water classes outside forested areas (see Table 1). Applications included carbon flux up-scaling [49], as well as up-scaling of soil carbon estimates [50]. Heikkinen et al. [49] grouped the original set of classes into seven new classes for one of the sub-basins: wet peaty tundra, dry peaty tundra, peat plateau, tundra heath, willow dominated stand, lake and pond margins and thermokarst lakes and profundal. Landsat TM classes were eventually combined with a high spatial resolution QuickBird image for a subset of the area [25]. The same thematic vegetation classes have been used in a nested approach. The original classes by Virtanen et al. [38] were grouped into peat plateau, fen, tundra heath, shrub tundra, willow/meadow and forest in order to use them as a proxy for soil properties. The application of the same QuickBird map was also demonstrated for up-scaling of carbon dioxide fluxes [51]. An interesting aspect of that study, beyond land cover mapping, is the description of the close relationship between the leaf area index and carbon dioxide fluxes. Finally, the Landsat land cover map of the northern part of the basin has also been assessed for the application of the up-scaling method to the circumpolar domain [52], where the spatial resolution was artificially reduced to simulate the use of vegetation products from the MODIS sensors and existing global land cover products. The land cover mapping accuracy was significantly lower due to the characteristic small patch size of land cover in these areas. Peat plateaus form however relatively homogeneous areas and contain the majority of soil carbon. It is suggested that the forest land cover classes, as well as willows and meadows are merged, as this procedure would have no considerable effect on the overall estimates. It was thus concluded that coarse resolution peatland maps can be nevertheless of value for soil carbon up-scaling. The issue of patch size has also been addressed by Virtanen and Ek [7] who compared different land cover classifications from QuickBird, ASTER and Landsat TM5. It was concluded that specifically water bodies and fens are problematic in medium resolution classifications, as they occur in the landscape in small or elongated patches and, thus, cannot be realistically classified from larger pixel sized images.

3.2. Further Studies

Other regions where satellite data classifications have been used for upscaling purposes are Zackenberg on Greenland, Svalbard and Kytalyk in Russia. Jorgensen et al. [53] used the classes dry tundra, moist tundra, fen and wet grassland derived from Landsat TM normalized difference water index composites to estimate fluxes in the Zackenberg valley, Greenland, in 2015. A more detailed, earlier classification by Elberling et al. [54], which was made for analyses of soil properties from airborne data, was used as the training dataset. This map also served as input for an estimate of soil organic carbon [55]. A similar upscaling method, but using GeoEye satellite images, has been applied over Kytalyk using a maximum-likelihood approach for the retrieval of land cover classes [56]. A vegetation map from Landsat TM/ETM+ has also been developed for Svalbard [57]. It was used for the selection of regions suitable for phytomass retrieval from NDVI over the Nordenskjöld peninsula [58]. A further subarctic study in northern Finland utilized high spatial resolution IKONOS data [59]. The classes mire, deciduous forest, evergreen forest, tundra and bare rock and lakes were

considered to characterize an eddy-flux tower footprint. The up-scaling is limited to the extent of the satellite image in that case.

4. Permafrost Subsurface and Land Surface Features

The application of land cover classifications has also proven significant for the retrieval of permafrost-related features. Specifically, thermokarst-related phenomena are studied, but periglacial processes in mountainous terrain have also been of interest. Many of these applications combine remotely-sensed terrain data with land cover information, e.g., [60–62]. Vegetation coverage provides information on process activity (erosion). Changes in hydrology due to permafrost degradation can be obtained from water body classifications [63]. Related features are in general rather small; the availability of high spatial resolution satellite data has therefore been the main driver for recent studies. Long-term studies are still limited. General process domains can however be captured using medium resolution datasets [62].

Morgenstern et al. [60] performed morphometric analyses of lakes based on Landsat-7 ETM+ in the Lena Delta. Landsat-7 ETM+ has also been used for the quantification of thermokarst-affected terrain types [64]. Ulrich et al. [65] used a combination of Landsat ETM+ (15 classes) and CHRIS-Proba (six classes) for spectral characterization of periglacial surfaces and retrieval of geomorphological process areas. Landsat 5 TM was applied by Turner et al. [66] in 2014 for identifying relations between catchment land cover characteristics and lake hydrology, concluding that remote sensing data alone cannot answer the related questions. Aeolian soil erosion, which can also be responsible for erosional landforms, or deflation patches have been studied in Kangerlussuaq, West Greenland [67], as well as the Yamal peninsula in Russia [68]. In both cases, high resolution satellite data were analyzed (WorldView-2 and GeoEye-1, respectively). Beck et al. [69] concluded that only high resolution satellite data can be used to map changes of so-called lithalsas. These are low, circular or oval features around 10–30 m wide and up to 150 m long that result from frost heave and are therefore permafrost-related surface features. High spatial detail is also required for ice wedge mapping. Liljedahl et al. [63] investigated high resolution satellite data from IKONOS, Corona, Gambit KH-7, QuickBird, WorldView-1/-2, SPOT 6/7 and aerial photographs to study ice wedge degradation across the Arctic, where changes over long time periods could be quantified.

The discrimination of lakes has been identified as a major challenge. Optical data can be easily used to identify lakes that are larger than the sensor's spatial resolution. Muster et al. [35] used CHRIS-Proba and Landsat-7 ETM+ to investigate subpixel-scale heterogeneity with special emphasis on Evapotranspiration (ET) estimation. Environments with inundated low centered polygons have been shown to be only detectable with high spatial resolution data. The majority of lakes are however smaller than, e.g., Landsat or MODIS, which are used for global maps [6,35], and frequent cloud cover limits the mapping of these highly dynamic features. SAR data have been suggested to overcome the latter problem. Large areas could be theoretically covered, but wind action, which is common in the Arctic, roughens the lake surface and reduces the detectability [36]. In the case of low wind conditions, higher spatial resolution X-band SAR data (2 m) have been shown to be applicable to capture small lake objects [70]. They provide more realistic representation of lakes than with Landsat as used for the regional map of the entire Lena Delta (see Table 1 [40]).

Land cover is also used to indirectly map sub-ground permafrost properties. ALT estimates have been made using different approaches, both by evaluation of land cover classifications, as well as by analysis of reflectance values themselves. In this context, there is also potential for X-band SAR applications to infer ALT from the radar backscatter, since the backscatter signal is strongly related to land cover [71]. Ou et al. [72,73] used Landsat-5 TM, as well as Radarsat-2 (C-band SAR) for permafrost modeling. A land cover map was produced, and values for peat thickness and vegetation height were associated with the resulting classes. Ground temperatures have been up-scaled using an ecotype land cover map (from among other sources, Landsat, stratified NDVI and unsupervised classification of Jorgenson et al. [74]) on a regional scale [75]. The available classes were grouped

into four clusters representing certain ground temperature ranges in a permafrost transition zone in Alaska. Ecotypes with thick moss and organic layers dominate the group with lowest temperatures, whereas thinner organic layers can be found at the warmer sites. Sites with mean annual ground temperature above zero degrees are sites with alder, spruce and also burned areas. A potential information source on organic layer properties is also C-band SAR, as measurements under frozen conditions reflect soil organic carbon content north of the treeline [76]. Extent mapping of peatland with C-band SAR (unfrozen period) has been shown in numerous studies (e.g., [77,78]). It is assumed that the near surface is comparably wet. An alternative approach is to take advantage of the backscatter signal arising from frozen surface conditions, which can provide general information on wetland distribution with up to four classes [79].

Land cover serves also as input for permafrost modeling, including semi-empirical equilibrium models [1]. It has strong implications for the small-scale distribution of the snow cover. Westermann et al. [1] reclassified a MODIS land cover product into high vegetation/forest (“International Geosphere-Biosphere Programme” (IGBP) Classes 1–9, 11) and bare ground/low vegetation (IGBP Classes 10, 15, 16). Areas with bare ground or low vegetation are locations where strong redistributions of snow due to wind drift can occur. Snow cover is more uniform in areas with trees and high vegetation. In some areas the model failed to reproduce the permafrost patterns. Especially the patchiness of shrublands cannot be resolved. Westermann et al. [1] suggest that subsurface properties should also be considered to better estimate the active layer damping factor. Selkowitz [80] has defined the class ‘shrub’ as vegetation that is less than 0.5 m tall. This specification is supposed to reflect certain properties, such as trapping by snow, where the threshold represents the approximate height boundary between shrubs that extend significantly above tussocks and shrubs that grow primarily between tussocks [80]. To better understand changes in permafrost temperatures, information on snow cover extent and depth, including redistribution potential and nival traps, is imperative. Not unexpectedly this demands clear delineation of assorted vegetation types through appropriate thematic detail.

5. Changing Land Cover and Transition Zones

Land cover change in high latitudes is mostly associated with shrub expansion, forest fires, thaw lake variations, grazing or settlement development (e.g., [81,82]). Change can be identified using, e.g., post-classification approaches or assessing trends of the measured reflectance. The latter yields especially large potential, since it avoids the problem of classification accuracy. The review of Stow et al. [83] in 2004 focused on land cover change in Arctic Tundra ecosystems. A number of selected studies has been summarized demonstrating various approaches with one example for each type of data: repeat terrestrial photography, aerial photography, high, medium and coarse resolution satellite image analyses. Land cover change from satellites is quantified based on indexes rather than classifications in all examples.

AVHRR NDVI is commonly used for pan-Arctic assessment [84,85], but Landsat on the regional scale. Especially the latter points to varying patterns across the Arctic. Greening is associated with lowland areas in Canada [86], but the opposite case is in Siberia where upland areas have been linked to positive NDVI trends [87]. This upland greening in the Urals, Gydan and Taymyr regions seems to be strongly connected to cryogenic disturbance processes in areas of patterned ground. According to Frost et al. [87], this is not captured by AVHRR analyses due to the limited size of single disturbance sites. The applicability of various further indexes has been demonstrated by Fraser et al. [88], who used pixel-based trend analysis of long-term Landsat TM/ETM+ image stacks to map gradual, long-term changes to vegetation (TC brightness, greenness and wetness indexes and fractional land cover trained from IKONOS high resolution images). Nitze and Grosse [89], Raynolds and Walker [90] confirmed the suitability of such an approach in the Lena Delta and on the Alaskan North Slope, respectively. These regions coincide with two of the areas with multi-purpose land cover mapping (see Figure 1). The advantage of Landsat is its potential for regional to global mapping and records longer than

30 years, which are especially exploited for water area changes (e.g., [81,91]). However, not only the spatial resolution, also the interpretation of water surface changes is challenging due to the inconsistent data coverage. NDVI trends are also interpreted for wetting and drying [89,92]. A general constraint for all Landsat-based approaches is the lack of data for 1989–1998 for much of the Arctic [87]. To capture and interpret subtle changes, high resolution satellite images are required [85,87].

A further challenging task is the detection of the tundra-taiga transition area. This is of specific interest to long-term studies on land cover change. Earlier studies, such as by Silapaswan et al. [93] in 2001, concluded that a combination of index analyses and unsupervised classification performs best. A hybrid unsupervised-supervised classification has been suggested by Rees and Williams [94] in 1997 to study the effect of air pollution on the Kola peninsula. Tundra and forest areas were analyzed by unsupervised classification separately. Their separation however is based on supervised classification. This approach results in classes that can be well distinguished rather than targeting predefined purpose-driven classes. Separate parametrization is however required for each scene. A similar approach was applied for the same purpose by Tommervik et al. [95].

Ranson et al. [96] found that methods using multi-spectral Landsat ETM+ summer images, multi-angle MISR red band reflectance images, RADARSAT images with larger incidence angle or multi-temporal and multi-spectral MODIS data provide similar classification results (supervised) over central Siberia for a certain date. Hufkens et al. [97] validated a sigmoid wave curve fitting algorithm to detect and quantify a forest-tundra ecotone based on Landsat ETM+ data in the Northwest Territories, Canada. The evaluation of a global forest cover map based on Landsat showed that forests closely matched canopies of at least 2 m in height in the tundra-taiga transition zone [98]. Apart from distinguishing forest from non-forested areas, shrubs were studied in the transition zone. Beck et al. [99] applied a random forest approach to map small and tall shrubs (>1 m) as their distribution reflects climatic conditions. Very high resolution datasets reveal shrub encroachment on disturbance sites [87].

The tundra-taiga transition area is also of interest to reindeer herding. Pastures, especially the abundance of lichens, have therefore been investigated with satellite data. For herding purposes, winter and summer pastures (different vegetation communities as a proxy for certain lichen types, on trees or within tundra heath) have been distinguished by Bartsch et al. [100] applying supervised (maximum-likelihood) classification. Hybrid classification has been used by Rees et al. [101] and Tommervik et al. [102] for grazing impact assessment. Grazing impact has also been addressed by the analysis of the fractional coverage of fruticose lichens with supervised (maximum-likelihood) classification [103].

6. National- and Regional-Scale Land Cover Maps

The main sources of regional- and/or national-scale land cover images are Landsat data. A special characteristic of such maps is that they are usually a combination of data from several years in order to achieve complete spatial coverage; e.g., Cihlar et al. [104] compiled a Canada-wide map fuzzy K-means clustering with 30-m resolution from three years of data. To some extent, information from coarser datasets, which are also used on the global scale, is applied.

Unsupervised classification with a preceding mosaicking step is commonly used for regional-scale mapping. Such an approach has been, e.g., also used for the first map of Northern Alaska based on Landsat MSS [46]. Landsat was also combined with e.g., SPOT VGT for normalization [8,105] in order to create a land cover map for the Canadian Northern Territories. IKONOS was utilized to develop an approach that provides land cover fractions within the Landsat resolution cells [24]. The national land cover map of the U.S. (from Landsat TM/ETM+) has been assessed regionally by Selkowitz and Stehman [106] over Alaska. An agreement of 59.4% for Level II (highest thematic detail) was found. This result underlines the need to address high latitude environments separately.

A different scheme has been adopted by Gould et al. [107,108]. NOAA-AVHRR data (1 km, including multi-temporal NDVI 10-day composites) are processed for Canada [107,108]. Polygons were

hand-drawn based on visual interpretation of variations in the AVHRR base map and interpretation of ancillary data. This strategy corresponds to the one chosen for the production of the Circum-Arctic Vegetation Map (CAVM; Figure 2) from NOAA-AVHRR [5,109], which was the first attempt to produce a consistent map with the necessary thematic content for vegetation studies. Only regional maps existed before [4]. Many studies have shown that the CAVM is the best regional-scale land cover product in the Arctic; e.g., Rees and Danks [110] have demonstrated its prevailing performance over global land cover maps for reindeer pasture mapping; however, it still lacks the necessary detail regarding separation of lichen- and shrub-dominated land cover types. A further constraint is its limitation to non-forested areas.

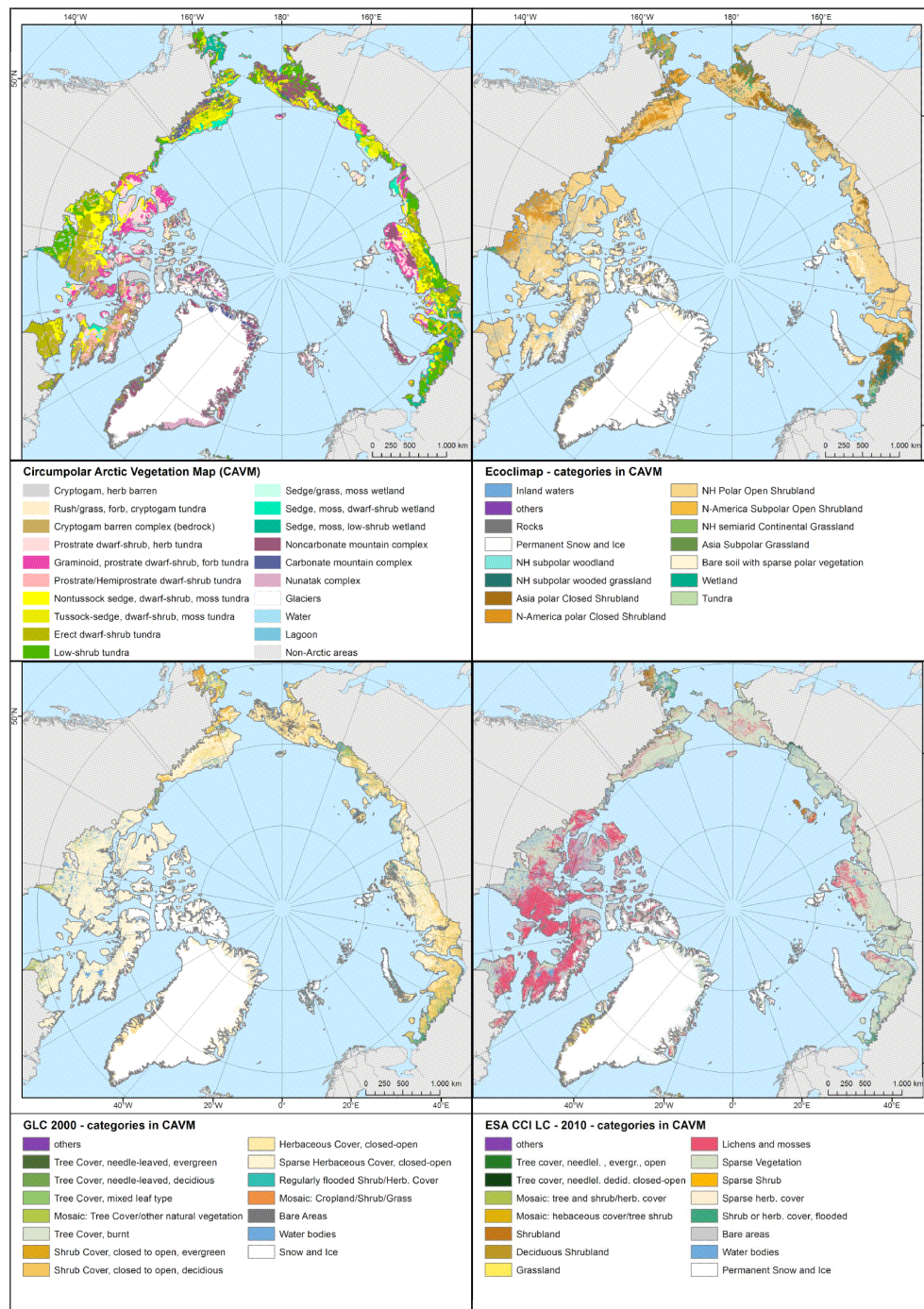


Figure 2. CAVM [5] and global land cover maps for the CAVM domain. For a description, see Table 2.

A range of approaches and sensors has been tested for Northern Eurasia, including usage of seasonal mosaics of SPOT4-VEGETATION (1 km, [111]), MODIS (500 m, [112]) and even radar data [113] from JERS-1 (L-band SAR, 100 m). This sensor is specifically suited to detect wetlands, as demonstrated by Whitcomb et al. [114]. Bartalev et al. [111] applied unsupervised ISODATA classification to SPOT data, Sulla-Menashe et al. [112] and De Grandi et al. [113] a maximum likelihood supervised scheme to JERS-1 and MODIS, respectively. One major issue of SPOT-4 products for applications in the Arctic is their spatial limitation to areas south of 70 degrees latitude. The random forest approach, which also utilizes training data, has been applied by Whitcomb et al. [114] to L-band SAR data. This approach proved to be especially applicable to wetland mapping.

SAR-based land cover maps have until recently only been based on summer (unfrozen condition) acquisitions. Widhalm et al. [79] demonstrated that winter C-band backscatter reflects certain land cover characteristics, especially wetlands. The 1-km SAR data better represent wetland spatial distribution than global maps, which have been developed from MODIS or MERIS (500 m and 300 m, respectively). The SAR data provide mostly surface roughness and only to a limited amount of volume scattering in vegetation in tundra regions. Traditional global maps include only classes for flooded shrublands. There is, however, a much higher diversity in wetland types across the Arctic. A common feature is the low surface roughness with respect to C-band (5.6-cm wavelength). One cannot obtain different types of wetlands with this approach, but their presence can be detected (at least four-times more than in global maps). This method can also potentially be applied to higher spatial resolution C-band SAR data as, e.g., available from Sentinel-1.

An alternative, a rather coarse (74 km × 43 km footprint) passive microwave dataset was produced by Melentyev and Matelenok [115] for latitudinal discrimination of Siberian landscapes using AMSR-E brightness temperature. A consistent threshold classification on the basis of seven informative features is suggested. Eight landscape types, which also include the boreal biome, could be distinguished: wetland complexes, tundra, transition regions, tundra-forest, forest-steppes, steppes, deciduous and mixed forest and taiga.

7. The Arctic in Global Land Cover Maps

The Arctic plays an important role for the global climate. Sustained increases in air temperatures are warming the Arctic more than twice as fast compared to low/mid-latitudes [116]. Rapid changes in the Arctic system feed into the global climate. The Arctic therefore needs to be addressed in its entirety rather than simply regionally. The impact of climate warming on permafrost and associated carbon fluxes is one of the issues addressed in current climate (land surface) modeling studies [3]. Land cover is required for benchmarking and initializing Earth system models. Such datasets are also required for large-scale numerical permafrost modeling [1]. A further potential application at this scale is up-scaling of carbon pools in permafrost areas. It has been shown in a range of studies that high resolution data can be used at the regional scale [25]. Land cover classes need to reflect certain land cover types that are associated with a certain Soil Organic Carbon Content (SOCC) range. The thematic detail for this application is missing in global maps to date. An alternative approach that does not require land cover classification has been developed by Bartsch et al. [76]. SOCC has been directly derived from C-band SAR backscatter. C-band SAR may thus provide complementary information to optical data on soil properties. Organic carbon content has a significant impact on the thermal properties of the soil, information required for permafrost modeling.

Global land cover maps are based on AVHRR ([117,118] IGBP DISCover and UMD maps), MODIS [119,120], SPOT 4 VEGETATION ([121] GLC2000), ENVISAT MERIS ([122,123] GlobCover and subsequent CCI maps) and recently also Landsat (e.g., Globland30 by the National Geomatics Center of China [124]). Existing land cover and seasonal datasets (from AVHRR) have been used to produce the ECOCLIMAP [125,126], a dataset developed for climate modeling purposes. The GlobCover and CCI maps are based on bi-monthly, seasonal and annual mosaics [122,123]; ECOCLIMAP on eight years of NDVI time series (see also Table 2).

Classes representing Plant Functional Types (PFTs) are required by Earth system models to define the vegetation characteristics in terms of, e.g., photosynthesis capacity, phenology and roughness [3]. The spatial resolution has been shown to be a clear advantage of GlobCover compared to GLC2000 by Otle et al. [3]. GlobCover tends to have better distributions of tree cover, but may lead to overestimation of forest PFTs. Otle et al. [3] suggested the use of additional information to address this issue. The opposite seems to be the case for the other maps. An assessment of the IGBP DisCover and MODIS land cover map over the West Siberian Lowlands demonstrated that at high latitudes, both underestimate deciduous needle-leaf forest in favor of woody savannas or open shrublands, respectively [127]. The transformation to PFTs by Otle et al. [3] using GlobCover led to an increase of bare soil in vegetated tundra areas in Siberia (except for Taymir) compared to a previous definition for the model ORCHIDEE.

The spatial resolution poses a major constraint for the applicability of coarse resolution data, such as AVHRR, MODIS and MERIS, in the Arctic. This is apparent and has been demonstrated for the water class [6,127]. Insufficient thematic detail for reindeer pasture mapping has also been demonstrated for the GLC2000 by Rees and Danks [110]. An option is the retrieval of the water fraction, which can be obtained by the fusion of datasets of different temporal and spatial resolution (e.g., [128] 5 km, AMSR-E and MODIS). Such approaches do, however, not provide information on lake objects as required for, e.g., thermokarst lake studies.

Global land cover maps are mostly produced by variants of unsupervised classification approaches. Table 2 provides details on the input data, method and validation of ECOCLIMAP-, GLC2000- and the MERIS-based land cover maps. They are shown in Figure 2 over the extent of the CAVM. Figures 3–5 provide a direct comparison of their classes with the CAVM. ECOCLIMAP contains significantly more global classes than the other maps, which use the FAO system. Their number is however similar in the Arctic domain. The actual thematic detail is lower for ECOCLIMAP, as it provides separate classes for North America and Asia for the same land cover type, but it is the only map that includes a tundra class. This class covers however only a very small proportion within the CAVM domain.

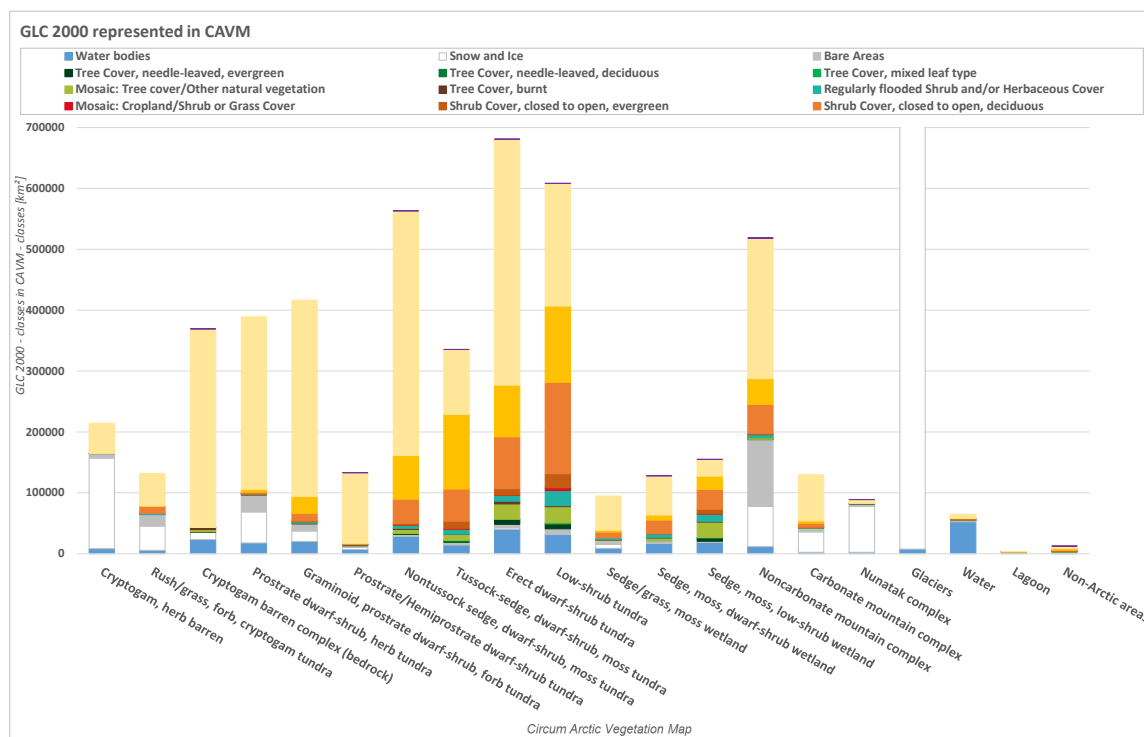


Figure 3. Comparison of GLC2000 classes with CAVM [5].

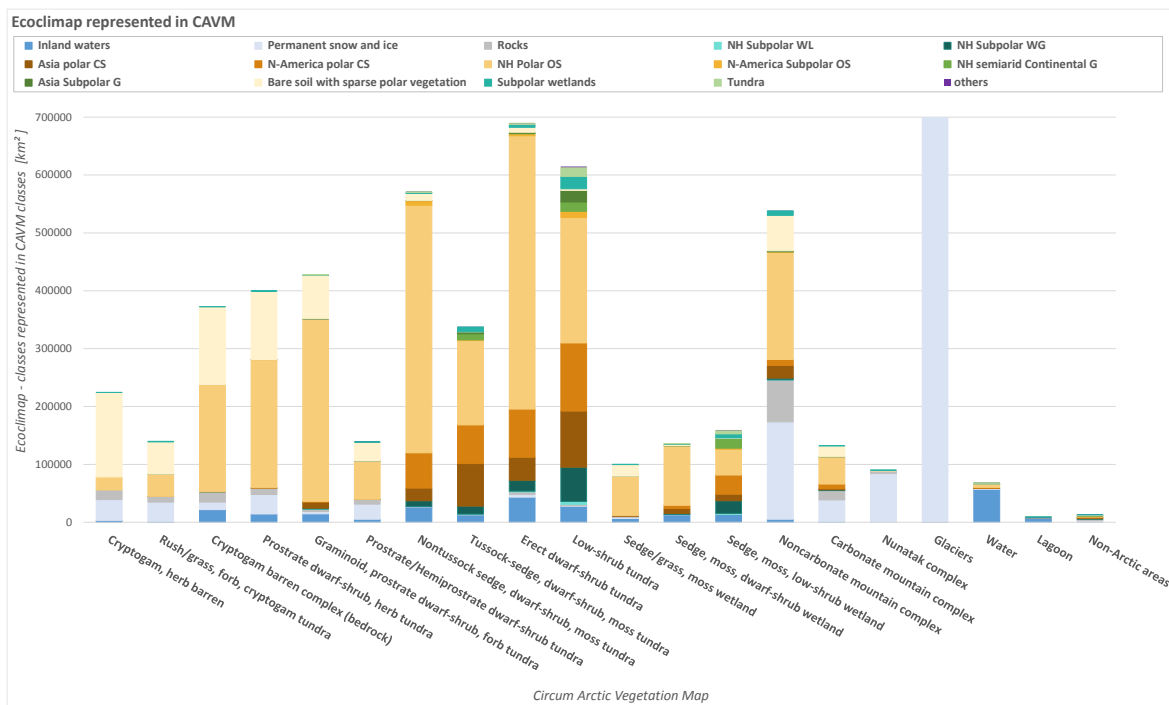


Figure 4. Comparison of ECOCLIMAP classes with CAVM [5].

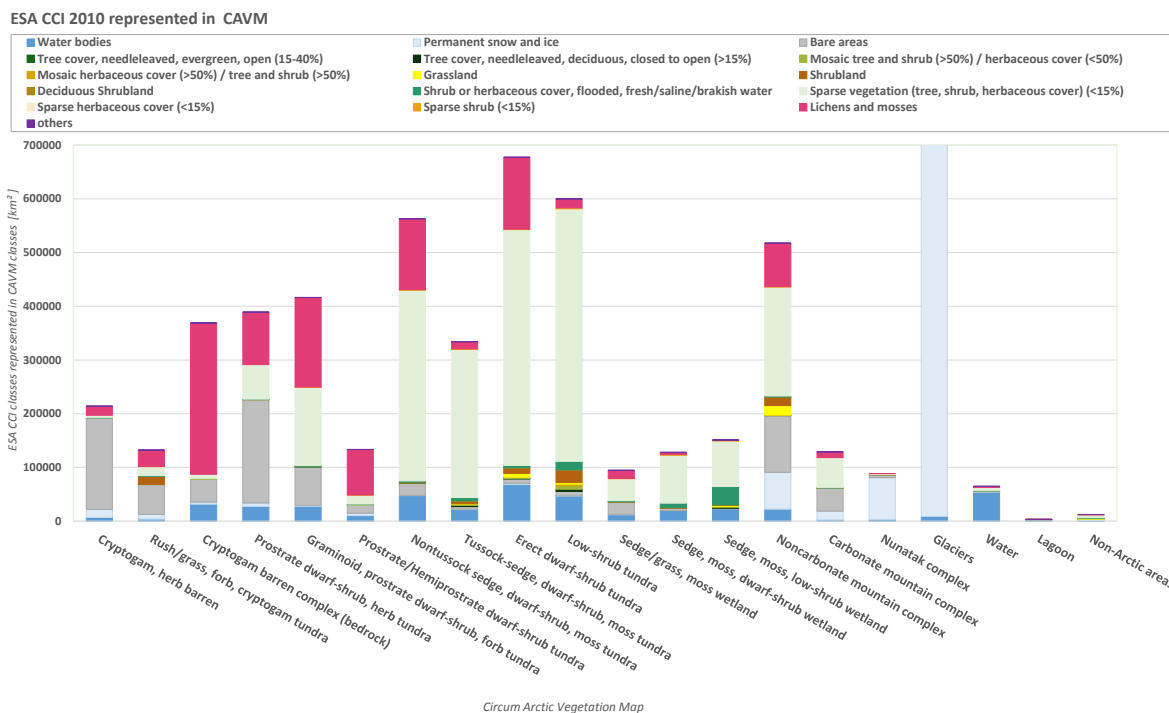


Figure 5. Comparison of CCI Land Cover 2010 classes with CAVM [5].

It has been demonstrated that global land cover datasets disagree especially in the transition zone from boreal to tundra [129,130]. Furthermore, the classes bare and shrub covered have been differently assigned [129]. This has been demonstrated when compared to selected Landsat-based land cover maps. It has also been pointed out by Westermann et al. [1] that shrublands cannot be resolved in coarse resolution global maps.

Already a visual comparison of the CAVM with global maps demonstrates the limited thematic content of global maps in the Arctic (Figure 2). The classes available from the CAVM (which represent vegetation communities) show largely different spatial patterns than the classes in the global maps, as they differ significantly by their definition (Table 3). The CCI land cover product has received increasing attention in recent studies. It includes a high latitude dedicated ‘mosses and lichens’ class. The full name is ‘closed to open (>15%) herbaceous vegetation (grassland, savannas or lichens/mosses)’. It is expected by users that mosses and lichens have a certain thickness and are cooling the ground [131]. This class corresponds however largely to mountain complexes with cryptogam crusts over the CAVM domain in the CCI map. These are very thin and often show a large active layer thickness [68,71]. A large proportion of this class also corresponds to dwarf shrub tundra, mostly of the graminoid type (see Figure 5). Lichens and mosses can be found within most land cover types in the high latitudes [100]. The species composition and amount differ between vegetation communities. A certain lichen coverage is associated with land cover types that can be identified with Landsat. Nordberg and Allard [103] demonstrated that lichen coverage increases reflectance across all Landsat channels. The higher the reflectance, the higher the lichen coverage. Grazing reduces the lichen height and, thus, also reflectance [95]. Large areas are affected by reindeer herding, as well as wild herds.

Thematic detail with respect to shrubs is highest for the ECOCLIMAP map. It distinguishes between closed and open shrublands. The closed shrublands correspond mostly to dwarf and low shrub tundra. The majority of shrub categories of the CAVM are however classified as open shrubland, which can be found in almost all CAVM classes (Figure 4) and is also the most common one with 37%. The GLC2000 also separates herbaceous from shrub cover over the Arctic. The most dominant class is ‘sparse herbaceous or sparse shrub cover’ (about 40%; Figure 3). Similar classes are included in the CCI land cover legend, but not mapped over the Arctic. This class named ‘closed to open (>15%) (broadleaved or needle-leaved, evergreen or deciduous) shrubland (<5 m)’ can be found in steppe zones and covers large areas of the Tibetan plateau, which is also a permafrost-affected region. Moreover, Western Greenland is inconsistent with the Arctic class pattern in the CCI product. It is the only region in the Arctic mapped as grassland. The majority (approximately 33%) is mapped as sparse vegetation (with less than 15% vegetation coverage). Although dominant classes are similar in quantity across the different maps, they overlap only partially. Water surfaces in all global maps are better resolved than in the CAVM.

Table 3 lists classes of the global maps, as well as CAVM within the extent of the multi-purpose maps described in Section 3. This exemplifies the large difference of the type of classes available in these maps. The dominating class (more than 20% coverage) in the CAVM differs among the three locations. The Usa basin is dominated by low shrubs, Kugaruk by tussocks, sedges and shrubs and the Lena Delta by graminoids, shrubs and forbs and wetlands with sedges. The CAVM agrees well over Kugaruk, as this has been the initial study site of the CAVM team. The dominating land cover also matches for the other two sites. The differences between the sites are not well represented in the global maps. The CCI land cover provides only one type of dominating land cover across the sites. ECOCLIMAP comes closest to the CAVM, but addresses the classes rather by vegetation structure, than with detail on actual vegetation communities. The GLC2000 reflects the transitional nature of the Usa basin. None of the global map represents the thematic content of the Landsat-derived regional maps (Table 1).

Table 2. Details of selected global land cover maps and CAVM. The number of classes refers to none-water/ice classes >1% within CAVM (total).

	ECOCLIMAP II	GLC 2000	ESA CCI Landcover	CAVM
Time	1999–2003 (multiannual)	2000	5 years centered on 2000/2005/2010	1993, 1995
Input data	SPOT Vegetation	SPOT 4 (Vega2000)	MERIS, SPOT, AATSR	AVHRR
Legend	LCCS (FAO)	LCCS (FAO)	LCCS (FAO)	dominant PFT, stature of woody shrubs (Walker et al. [5])
Classes	6 (273)	6 (22)	5 (37)	16 (19)
Origin	Meteo France	JRC	ESA	USFWS, CAFF
Strategy	ECOCLIMAP II uses the information contained in multiannual SPOT/VEGETATION, NDVI profiles to split LC classes in more homogenous sub-classes	Ad hoc processing, relying on a multiple thematic approach, subtractive based on LCCS (FAO)	Designed to be globally consistent while regionally tuned, developed with GlobCover [123] and MODIS knowledge	Integrates ancillary information and regional expertise of mapping scientist
Accuracy and validation procedure	input (LAI from NDVI) is validated against in situ ground observations	Overall ~68.6% (Mayaux et al. [132]); quality control by comparison with ancillary data and quantitative accuracy assessment based on stratified random sampling of reference data	74.1 % compared to GlobCover (Bontemps et al. [133]); carried out externally; new validation tool (online interface for experts) was developed	Accuracy Level = 67.10%; validated by experts in LC-regions
Spatial resolution	1 km	1 km	300 m	1 km, minimum polygon size 14 km
Processing chains	Combination of 15 Types of LC, described by satellite data and Köppen’s world climate classes to discriminate LC-types number of “possible ecosystems”; Main LC-types from Global land cover map (University of Maryland, Hansen et al. [118]) derived from NOAA/AVHRR; snow/wetlands from IGBP-DIS map (Loveland and Belward [134])	“regionally tuned” approach; different processing approaches according to the region: input data generation from multispectral and multitemporal datasets, fractional cover percentage or combination of multispectral and multitemporal data with additional indicators from time series	MERIS 10-year LC map as the baseline, SPOT time series for updating; three 5-year epochs centered on the years 2010 (2008–2012), 2005 (2003–2007) and 2000 (1998–2002)	A false color-infrared (CIR) image of AVHRR data was used as the base map for drawing map polygons (manual ‘photointerpretation’). The color for each pixel was determined by its reflectance at the time of maximum greenness.
Classification mode	Hybrid-unsupervised classifier using 8 years of NDVI; comparison of NDVI annual profiles: if more than one month separation of minimum (maximum), then no aggregation; if two NDVI profiles for two ecosystems of the same cover type are found on several continents, then aggregation	Homogenous classification procedure (IGPB), unsupervised classifier (ISODATA)	Unsupervised classification chain, but improved by adding machine learning classification steps and the multi-year strategy (bi-monthly, seasonal and annual mosaics)	Classification steps: 1. Per pixel: supervised classification, identifying LC-classes that are not well represented; unsupervised classes, creating clusters of similar pixels; 2. Per cluster: cluster grouping in spectro-temporal classes according to their similarity in temporal space
Literature	Masson et al. [125], Champeaux et al. [126]	Bartholome and Belward [121], Mayaux et al. [132]	CCI LC project [135]	CAVM Team [136]

Table 3. Non-water classes with more than 1% coverage of global land cover maps and CAVM within regions of multi-purpose land cover classifications. Dominating classes (more than 20%) are underlined. For the location, see Figure 1 and specifications Table 1.

Type	Usa Basin (Non-Forest Part)	Kuparuk Basin	Lena Delta
CAVM		Nontussock sedge, dwarf shrub, moss tundra	Prostrate dwarf shrub, herb tundra
		<u>Tussock sedge, dwarf shrub, moss tundra</u>	<u>Graminoid, prostrate dwarf shrub, forb tundra</u>
		Erect dwarf shrub tundra	Nontussock sedge, dwarf shrub, moss tundra
		<u>Low shrub tundra</u>	Erect dwarf shrub tundra
		Sedge, moss, low shrub wetland	Low shrub tundra
		Non-carbonate mountain complex	Sedge/grass, moss wetland
		Carbonate mountain complex	<u>Sedge, moss, dwarf shrub wetland</u>
ECOCLIMAP		Carbonate mountain complex	Non-carbonate mountain complex
		Boreal evergreen needle-leaved forest	
		NH sub-polar mixed forest	
		NH sub-polar woodland	
		<u>NH sub-polar wooded grassland</u>	<u>North America polar closed shrub</u>
		Asia polar closed shrub	Asia polar closed shrub
		NH polar open shrub	<u>NH polar open shrub</u>
GLC2000		Asia sub-polar grassland	
		Tree cover, needle-leaved, evergreen	
		Mosaic: tree cover/other natural vegetation	Mosaic: tree cover/other natural vegetation
		<u>Shrub cover, closed-open, deciduous</u>	Shrub cover, closed-open, evergreen
		Herbaceous cover, closed-open	Shrub cover, closed-open, deciduous
		Sparse herbaceous or sparse shrub cover	Herbaceous cover, closed-open
		Regularly flooded shrub and/or herbaceous cover	<u>Sparse herbaceous or sparse shrub cover</u>
CCI Landcover		Bare areas	Bare areas
		Tree cover, needle-leaved, evergreen, closed to open (>15%)	Tree cover, needle-leaved, deciduous, closed to open (>15%)
		Mosaic tree and shrub (>50%)/herbaceous cover (<50%)	Lichens and mosses
		<u>Sparse vegetation (tree, shrub, herbaceous cover) (<15%)</u>	<u>Sparse vegetation (tree, shrub, herbaceous cover) (<15%)</u>
Regional map dom. class		Shrub or herbaceous cover, flooded, fresh/saline/brackish	Shrub or herbaceous cover, flooded, fresh/saline/brackish
		Bare areas	Bare areas
	Dwarf shrub moss tundra heath	Moist graminoid, prostrate shrub tundra	Wet sedge- and moss-dominated tundra

8. Challenges and Promising Approaches

There is a range of comparison studies of different methods for land cover classifications in high latitudes. These are usually limited to small areas. Land cover change is mostly addressed on the local scale. Classifications of land cover types other than water surfaces have only rarely been used for change detection in Arctic environments, except for identifying disturbances, such as air pollution or grazing effects. Indexes are commonly used to address land cover change issues. Classifications are however of benefit for identifying the tundra-taiga transition zone, which is of special interest to climate change impact studies.

Radar (SAR)-based large-scale maps often use supervised approaches, optical mostly unsupervised. Unsupervised classifications are also the basis for national to global mapping. Single purpose-driven maps are prepared with a priori information applying supervised classification approaches, such as data on the impact of air pollution and reindeer pasture inventories, or the maps are made manually, like the CAVM by Walker et al. [5]. The latter is widely used and based on AVHRR data. Object-based Image Analysis (OBIA) is a frequently-used approach classifying high resolution satellite data in general, but has little importance for applications in the high latitudes. That might be due to the fractional nature of the landscape and limited occurrence of artificial objects. Settlements are only rarely studied with land cover maps. This might however become more important in the future due to an increasing need for climate change impact assessments on local communities.

Different applications require to some extent varying spatial and thematic detail (Figure 6). Habitat studies have mostly been made with respect to mammals. Medium spatial resolution maps, which can be supplied by Landsat, are widely used. Mostly six to eight classes are derived. The required thematic detail increases with decreasing spatial resolution in the case of soil carbon, carbon flux, permafrost surface features and water cycle applications. Medium resolution data studies usually cover larger areas and therefore include a higher diversity of relevant landscape units. This implies that a higher thematic content is required from global maps than currently available. For the application of a resolution of 20–30 m (as available from, e.g., Landsat and also Sentinel-2) on average seven classes are common for regional applications. The CAVM also provides six to nine non-water classes for specific regions (see Table 3). However, twelve distinct classes are already required to represent the three featured multi-purpose maps together across the Arctic. Past studies on indirect assessment of permafrost subsurface features partially use a rather low number of classes, which are grouped from higher level detail maps. Even in the case of ten (surficial material) classes [73], a lower number is eventually relevant for permafrost-related classes, as they represented also non-permafrost types. This demonstrates that the potential of satellite data to conclude on sub-ground thermal properties is limited. Only general classes can be derived, and applicability has been proven in permafrost transition zones only. The relevant types are peatlands (with differentiation by vegetation cover) [73] and ecotypes that distinguish between low and tall shrubs, as well as their characteristic moss and organic layers [75]. This demand for details on shrubs coincides with statements in studies for numerical permafrost modeling [1,80]. They are important for the modeling of snow distribution (and subsequent impact on ground thermal conditions). A height threshold of 0.5 m is suggested for permafrost modeling purposes [106]. A range of recent publications on the use of polarimetric SAR data [31–33] has shown the potential of such data for shrub mapping, but the applicability remains limited since SAR data are only locally acquired in fully-polarimetric mode. Current acquisition strategies of SAR missions only provide equal and dual polarized data. Shrub mapping in general needs to consider phenological stages [20].

There is no generally agreed upon classification scheme for the northern high latitudes. Walker et al. [45] have also pointed this out as an issue for in situ mapping across the Arctic recently. Classes of regional maps for multiple purposes, such as up-scaling of carbon pools and fluxes, represent shrub physiognomy (dwarf species or higher) and wetness patterns. Shrubs are included as a class in global land cover maps, but are either not present in their Arctic parts or patterns differ among them. Wetlands or wetness descriptions are in general under-represented in global maps. They can have differing vegetation coverage. The same applies to lichens. They are omnipresent. Vegetation classes need to be reviewed and described for their associated lichens. The class 'lichens and mosses' in the CCI land cover can be interpreted as either cryptogam crust or graminoid dwarf shrub tundra. When lichen species are dominant and not covered by the canopy of higher vegetation, they are part of cryptogam crusts or develop within vegetation communities with graminoids. This should be labeled accordingly to avoid confusion with fruticose lichen heaths in boreal environments. Alternatively, lichens can be addressed by a vegetation community approach or by quantification of their bias on reflectance.

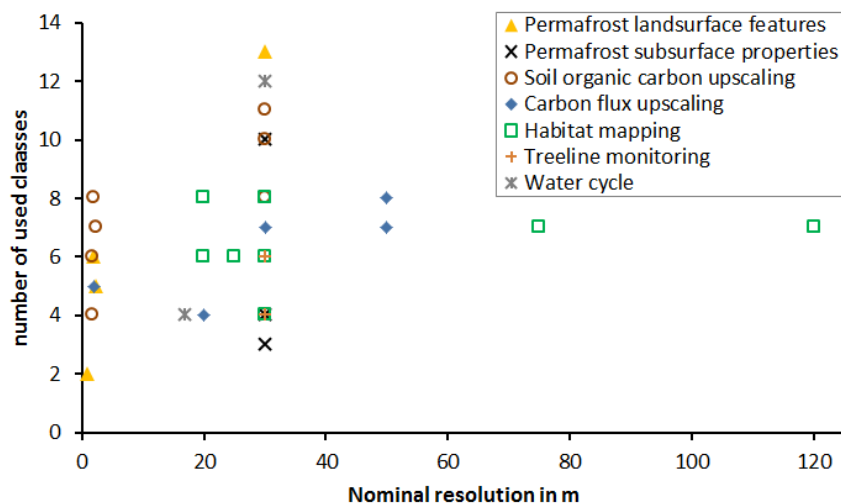


Figure 6. Comparison of the number of classes and spatial resolution from land cover classifications north of the treeline for different applications. (sources: [9,11,13,23,25,26,35,40–42,47,50,52,56,59,63,64,66,67,69,73,75,96,97,100–103,110]).

A good example for thematic content is the scheme developed by Gould et al. [108] for classification of Landsat data for Canada. Several graminoid and growth form dependent shrub classes are included. They specifically also address PFTs. In total, 17 PFTs are suggested for north of the treeline. The suitability of the suggested scheme for high latitudes, as well as the classification for Northern Alaska by Muller et al. [46] has been recently pointed out in a review by Wulschleger et al. [137]. Classes for high Arctic tundra are also suggested by Langford et al. [138] (graminoid types, lichens, mosses and forb). They are however derived using high spatial resolution (WorldView) data. The heterogeneous distribution of the PFTs can be captured at the local scale only. Time series representing phenology have been applied in all three cases [46,108,138].

Strategies for classifications on global and regional level differ regarding the type of input data. Acquisitions from several points in time are used also regionally, but seasonality is in general not considered. Global classification schemes make use of mosaics of different time intervals and comply with international classification schemes. These schemes do not reflect the diversity of landscape types in high latitudes, which are required in permafrost regions for common applications. Since global mapping efforts need to comply with internationally-agreed upon standards, only a substitution over the high latitudes, which is to some extent compatible with the global maps, can be made. Existing classes need to be re-named and subdivided. The same sub-class may have to be assigned to different parent classes eventually. This is, e.g., the case for wetlands. Alternatively, they could be provided as a separate information layer for the purpose of up-scaling of fluxes.

Global maps are in general based on optical data. Only SAR-based lake mapping has been so far considered in one case (CCI Landcover, [139]). SAR can, however, deliver similar thematic information content (e.g., [32,73]), especially when combinations of different polarizations are used. It provides additional information on surface roughness [76], moisture [78] and vegetation structure [140,141]. These parameters reflect information on wetlands [79], shrubs and soil properties which is required for high latitude applications. The thickness of mosses represents to some extent soil organic carbon content, and it relates to wetlands. C-band SAR has been shown to provide information on both in tundra areas. L-band SAR is also suitable for wetland mapping. A number of L-band maps already exist with a forest or wetland mapping focus for Northern Eurasia [113] and America [114]. They may need to be reviewed for consistency and harmonized, as well as gap filled across the Arctic. Such data could complement the traditional optical data-based retrieval methods. So far, mostly unfrozen period SAR data have been used. Recent studies demonstrated the potential of winter

acquisitions [76,79,140,141] for land surface characterization. The advantage is the exclusion of pixel to pixel variation, the difficult to model backscatter contributions due to differing dielectric properties when unfrozen [76]. Passive microwave data, such as AMSR-E, provide coarse resolution information on the water fraction [128], but also different land cover classes [115], including wetland complexes. Their resolution is similar to climate models, and wetland information is of need for land surface modeling in high latitudes [36]. Such maps would be therefore useful, but not applicable beyond. Medium resolution satellite data may, however, provide sufficient spatial resolution for soil properties up-scaling over peatlands [52]. On the local scale, X-band SAR, as well as UAVs become more and more important (e.g., [142–144]). Such investigations can complement regional mapping efforts in a nested approach in order to reflect the fragmented nature of permafrost regions and to identify the subtle changes at the land surface.

The majority of publications reviewed in this paper deal with retrieval techniques. Only about 40 of them make use of the classification results for, e.g., habitat mapping, soil carbon and flux upscaling or periglacial features detection (Figure 6). Most local and regional maps are not shared on online repositories. Exceptions are the CAVM [5], the Lena Delta map [40,145] and also the Kuparuk basin maps. This fosters their usage, but usually one of their co-authors is directly involved in new applications in case of regional maps. The CAVM has been used beyond the original development team due to its circumpolar coverage.

9. Conclusions

Global maps need to be conform with international classification schemes, which are of limited applicability in the Arctic. They might be to some extent suitable for treeline monitoring, but not for up-scaling or modeling to the north. New classifications that serve the needs at high latitudes need to be developed separately, but circumpolar and compatible with global maps. Existing methodologies for SAR data could be exploited to widen the thematic detail available from such maps. Winter, as well as summer acquisitions from C-band missions (e.g., Sentinel-1 and Radarsat) might be suitable to complement traditional classifications with C-band based approaches. A spatial resolution around 30 m has been shown suitable for a range of applications. This implies that the current Landsat-8, as well as Sentinel-2 missions would be adequate as input data.

Of special interest are shrubs and wetlands, as well as the occurrence of mosses and lichens. The identification of shrubs and their height is of interest to permafrost modeling, as this can serve as a proxy for snow distribution. The ‘shrub’ class is available in global land cover products, but it is not mapped at all, or not consistently, at high latitudes. Wetness, as well as moss and lichen coverage are in general sub-features across all traditional land cover classes and, therefore, mostly not used as separate classes in local to regional maps. The predominance of shrubs, tussocks and sedges provides the background information for purpose-driven classification schemes. This should be also considered for circumpolar mapping.

Acknowledgments: This study has been funded by the European Space Agency project DUE GlobPermafrost (Contract Number 4000116196/15/I-NB), which is lead by the Zentralanstalt für Meteorologie und Geodynamik. Further support was received by the Austrian Science Fund under Grant I1401. A.M. Trofaier was the recipient of a Research Fellowship by the European Space Agency’s Climate Office during the writing of the manuscript. We also would like to thank the four anonymous reviewers for their comments on the manuscript.

Author Contributions: A.B. developed the concept of the paper and wrote the majority of the manuscript. A.H. collected and categorized the literature reviewed in this paper. C.K. prepared all land cover figures and supported the global dataset review. A.M.T. contributed to the literature review and discussion in the manuscript.

Conflicts of Interest: The authors declare no conflict of interest. The funding sponsors had no role in the design of the study; in the collection, analyses or interpretation of data; in the writing of the manuscript; nor in the decision to publish the results.

Abbreviations

The following abbreviations are used in this manuscript:

ALOS	Advanced Land Observing Satellite
ALT	Active Layer Thickness
AMSR-E	Advanced Microwave Scanning Radiometer-Earth Observing System
ASTER	Advanced Spaceborne Thermal Emission and Reflection Radiometer
AVHRR	Advanced Very High Resolution Radiometer
CAFF	Conservation of Arctic Flora and Fauna
CAVM	Circum-Arctic Vegetation Map
CCI	Climate Change Initiative
CHRIS	Compact High Resolution Imaging Spectrometer
CS	Closed Shrubland
DCW	Digital Chart of the World
DIS	Data and Information System
DUE	Data User Element
EBF	Evergreen Broadleaf Forest
ENF	Evergreen Needle-leaf Forest
ENVISAT	Environmental Satellite
ERS	European Remote Sensing Satellite
ESA	European Space Agency
ET	Evapotranspiration
ETM	Enhanced Thematic Mapper
FAO	Food and Agriculture Organization
G	Grassland
GLC	Global Land Cover
GPP	Gross Primary Production
HRV	High Resolution Visible
IGBP	International Geosphere-Biosphere Programme
ISODATA	Iterative Self-Organizing Data Analysis Technique Algorithm
JERS	Japanese Earth Resources Satellite
JRC	Joint Research Centre
KH	Keyhole
LAI	Leaf Area Index
LC	Land Cover
LCCS	Land Cover Classification System
MERIS	Medium Resolution Imaging Spectrometer
MISR	Multi-angle Imaging Spectroradiometer
MODIS	Moderate Resolution Imaging Spectroradiometer
MSS	Multispectral Scanner System
NDVI	Normalized Difference Vegetation Index
NH	Northern Hemisphere
NOAA	National Oceanic and Atmospheric Administration
NPP	Net Primary Production
ORCHIDEE	Organizing Carbon and Hydrology in Dynamic Ecosystems
OS	Open Shrubland
PALSAR	Phased Array L-Band Synthetic Aperture Radar
PFT	Plant Function Type
Proba	Project for On-Board Autonomy
SAR	Synthetic Aperture Radar
SOCC	Soil Organic Carbon Content
SPOT	Satellite Pour l'Observation de la Terre
TC	Tasseled Cap
TM	Thematic Mapper
UMD	University of Maryland
VGT	Vegetation
WG	Wooded Grassland
WL	Woodland

References

1. Westermann, S.; Ostby, T.I.; Gislason, K.; Schuler, T.V.; Eitzelmueller, B. A ground temperature map of the North Atlantic permafrost region based on remote sensing and reanalysis data. *CRYOSPHERE* **2015**, *9*, 1303–1319.
2. Smith, M. Potential Responses of Permafrost to Climatic Change. *J. Cold Reg. Eng.* **1990**, *4*, 29–37.
3. Otle, C.; Lescure, J.; Maignan, F.; Poulter, B.; Wang, T.; Delbart, N. Use of various remote sensing land cover products for plant functional type mapping over Siberia. *Earth Syst. Sci. Data* **2013**, *5*, 331–348.
4. Walker, D.; Bay, C.; Daniels, F.; Einarsson, E.; Elvebakk, A.; Johansen, B.; Kapitsa, A.; Kholod, S.; Murray, D.; Talbot, S.; et al. Toward a new arctic vegetation map—A review of existing maps. *J. Veg. Sci.* **1995**, *6*, 427–436.
5. Walker, D.; Gould, W.; Maier, H.; Reynolds, M. The Circumpolar Arctic Vegetation Map: AVHRR-derived base maps, environmental controls, and integrated mapping procedures. *Int. J. Remote Sens.* **2002**, *23*, 4551–4570.
6. Bartsch, A.; Pathe, C.; Scipal, K.; Wagner, W. Detection of permanent open water surfaces in central Siberia with ENVISAT ASAR wide swath data with special emphasis on the estimation of methane fluxes from tundra wetlands. *Hydrol. Res.* **2008**, *39*, 89–100.
7. Virtanen, T.; Ek, M. The fragmented nature of tundra landscape. *Int. J. Appl. Earth Obs. Geoinf.* **2014**, *27*, 4–12.
8. Olthof, I.; Latifovic, R.; Pouliot, D. Development of a circa 2000 land cover map of northern Canada at 30 m resolution from Landsat. *Can. J. Remote Sens.* **2009**, *35*, 152–165.
9. Pearce, C. Mapping muskox habitat in the canadian high arctic with spot satellite data. *Arctic* **1991**, *44*, 49–57.
10. Markon, C.; Derksen, D. Identification of tundra land cover near Teshekpuk Lake, Alaska using SPOT satellite data. *Arctic* **1994**, *47*, 222–231.
11. Kayhko, J.; Pellikka, P. Remote sensing of the impact of reindeer grazing on vegetation in northern Fennoscandia using SPOT XS data. *Polar Res.* **1994**, *13*, 115–124.
12. Belchansky, G.; Ovchinnikov, G.; Douglas, D. Comparative evaluation of ALMAZ, ERS-1, JERS-I and Landsat-TM for discriminating wet tundra. In Proceedings of the 1995 International Geoscience and Remote Sensing Symposium, Quantitative Remote Sensing for Science and Applications (IGARSS 95.), Firenze, Italy, 10–14 July 1995; Stein, T., Ed.; Volume 1, pp. 309–311.
13. Belchansky, G.; Ovchinnikov, G.; Kozlenko, N.; Douglas, D. Assessment of dependence between SAR data focusing parameters and tundra habitat classification. In Proceedings of the 1995 International Geoscience and Remote Sensing Symposium, Quantitative Remote Sensing for Science and Applications (IGARSS 95), Firenze, Italy, 10–14 July 1995; Stein, T., Ed.; Volume 1, pp. 219–221.
14. Joria, P.; Jorgenson, J. Comparison of three methods for mapping tundra with landsat digital data. *Photogramm. Eng. Remote Sens.* **1996**, *62*, 163–169.
15. Rees, W.G. *Physical Principles of Remote Sensing*, 3rd ed.; Cambridge University Press: Cambridge, UK, 2013.
16. Mosbech, A.; Hansen, B. Comparison of satellite imagery and infrared aerial photography as vegetation mapping methods in an arctic study area—Jameson Land, East Greenland. *Polar Res.* **1994**, *13*, 139–152.
17. Brossard, T.; Joly, D. Probability models, remote sensing and field observation: Test for mapping some plant distributions in the Kongsfjord area, Svalbard. *Polar Res.* **1994**, *13*, 153–161.
18. Cihlar, J.; Ly, H.; Xiao, Q. Land cover classification with AVHRR multichannel composites in northern environments. *Remote Sens. Environ.* **1996**, *58*, 36–51.
19. Fleming, M.D. *The Second Circumpolar Arctic Vegetation Mapping Workshop, Arendal, Norway, 19–24 May 1996 and The CAVM-North American Workshop, Anchorage Alaska, US, 14–16 January 1997*; Institute of Arctic and Alpine Research: Boulder, CO, USA, 1997; pp. 25–26.
20. Walker, D. An integrated vegetation mapping approach for northern Alaska (1:4 M scale). *Int. J. Remote Sens.* **1999**, *20*, 2895–2920.
21. Liu, J.; Chen, J.; Cihlar, J.; Chen, W. Net primary productivity distribution in the BOREAS region from a process model using satellite and surface data. *J. Geophys. Res.-Atmos.* **1999**, *104*, 27735–27754.
22. Williams, M.; Rastetter, E.; Shaver, G.; Hobbie, J.; Carpino, E.; Kwiatkowski, B. Primary production of an arctic watershed: An uncertainty analysis. *Ecol. Appl.* **2001**, *11*, 1800–1816.
23. Takeuchi, W.; Tamura, M.; Yasuoka, Y. Estimation of methane emission from West Siberian wetland by scaling technique between NOAA AVHRR and SPOT HRV. *Remote Sens. Environ.* **2003**, *85*, 21–29.
24. Olthof, I.; Fraser, R.H. Mapping northern land cover fractions using Landsat ETM. *Remote Sens. Environ.* **2007**, *107*, 496–509.

25. Hugelius, G.; Virtanen, T.; Kaverin, D.; Pastukhov, A.; Rivkin, F.; Marchenko, S.; Romanovsky, V.; Kuhry, P. High-resolution mapping of ecosystem carbon storage and potential effects of permafrost thaw in periglacial terrain, European Russian Arctic. *J. Geophys. Res.-Biogeosci.* **2011**, *116*, G03024.
26. Broderick, D.E.; Frey, K.E.; Rogan, J.; Alexander, H.D.; Zimov, N.S. Estimating upper soil horizon carbon stocks in a permafrost watershed of Northeast Siberia by integrating field measurements with Landsat-5 TM and WorldView-2 satellite data. *Gisci. Remote Sens.* **2015**, *52*, 131–157.
27. Moody, D.I.; Brumby, S.P.; Rowland, J.C.; Altmann, G.L. Land cover classification in multispectral imagery using clustering of sparse approximations over learned feature dictionaries. *J. Appl. Remote Sens.* **2014**, *8*, doi:10.1117/1.JRS.8.084793.
28. Fraser, R.; McLennan, D.; Ponomarenko, S.; Olthof, I. Image-based predictive ecosystem mapping in Canadian arctic parks. *Int. J. Appl. Earth Obs. Geoinf.* **2012**, *14*, 129–138.
29. Atwood, D.K.; Small, D.; Gens, R. Improving PolSAR Land Cover Classification With Radiometric Correction of the Coherency Matrix. *IEEE J. Sel. Top. Appl. Earth Obs. Remote Sens.* **2012**, *5*, 848–856.
30. Banks, S.; Ullmann, T.; Roth, A.; Schmitt, A.; Dech, S.; King, D. Classification of Arctic Coastal Land Covers with Polarimetric SAR Data. In Proceedings of the 2013 IEEE Radar Conference (RADAR), Ottawa, ON, Canada, 29 April–3 May 2013.
31. Banks, S.N.; King, D.J.; Merzouki, A.; Duffe, J. Characterizing scattering behaviour and assessing potential for classification of Arctic shore and near-shore land covers with fine Quad-Pol RADARSAT-2 data. *Can. J. Remote Sens.* **2014**, *40*, 291–314.
32. Ullmann, T.; Schmitt, A.; Roth, A.; Duffe, J.; Dech, S.; Hubberten, H.W.; Baumhauer, R. Land cover characterization and classification of Arctic tundra environments by means of polarized synthetic aperture X- and C-band radar (PolSAR) and Landsat 8 multispectral imagery—Richards Island, Canada. *Remote Sens.* **2014**, *6*, 8565–8593.
33. Duguay, Y.; Bernier, M.; Levesque, E.; Domine, F. Land cover classification in SubArctic regions using fully polarimetric RADARSAT-2 data. *Remote Sens.* **2016**, *8*, 697.
34. Duguay, C.R.; Zhang, T.; Leverington, D.W.; Romanovsky, V.E. Satellite remote sensing of permafrost and seasonally frozen ground. In *Remote Sensing in Northern Hydrology: Measuring Environmental Change*; American Geophysical Union: Washington, DC, USA, 2013; pp. 91–118.
35. Muster, S.; Langer, M.; Heim, B.; Westermann, S.; Boike, J. Subpixel heterogeneity of ice-wedge polygonal tundra: A multi-scale analysis of land cover and evapotranspiration in the Lena River Delta, Siberia. *Tellus Ser. B-Chem. Phys. Meteorol.* **2012**, *64*, 17301.
36. Bartsch, A.; Trofaier, A.M.; Hayman, G.; Sabel, D.; Schläffer, S.; Clark, D.B.; Blyth, E. Detection of open water dynamics with ENVISAT ASAR in support of land surface modeling at high latitudes. *Biogeosciences* **2012**, *9*, 703–714.
37. Trofaier, A.M.; Bartsch, A.; Rees, W.G.; Leibman, M.O. Assessment of spring floods and surface water extent over the Yamalo-Nenets Autonomous District. *Environ. Res. Lett.* **2013**, *8*, 045026.
38. Virtanen, T.; Mikkola, K.; Nikula, A. Satellite image based vegetation classification of a large area using limited ground reference data: A case study in the Usa Basin, north-east European Russia. *Polar Res.* **2004**, *23*, 51–66.
39. Muller, S.; Walker, D.; Nelson, F.; Auerbach, N.; Bockheim, J.; Guyer, S.; Sherba, D. Accuracy assessment of a land-cover map of the Kuparuk River Basin, Alaska: Considerations for remote regions. *Photogramm. Eng. Remote Sens.* **1998**, *64*, 619–628.
40. Schneider, J.; Grosse, G.; Wagner, D. Land cover classification of tundra environments in the Arctic Lena Delta based on Landsat 7 ETM+ data and its application for upscaling of methane emissions. *Remote Sens. Environ.* **2009**, *113*, 380–391.
41. Reeburgh, W.; King, J.; Regli, S.; Kling, G.; Auerbach, N.; Walker, D. A CH₄ emission estimate for the Kuparuk River basin, Alaska. *J. Geophys. Res.-Atmos.* **1998**, *103*, 29005–29013.
42. Stow, D.; Hope, A.; Boynton, W.; Phinn, S.; Walker, D.; Auerbach, N. Satellite-derived vegetation index and cover type maps for estimating carbon dioxide flux for arctic tundra regions. *Geomorphology* **1998**, *21*, 313–327.
43. Nelson, F.; Shiklomanov, N.; Mueller, G.; Hinkel, K.; Walker, D.; Bockheim, J. Estimating active-layer thickness over a large region: Kuparuk River Basin, Alaska, USA. *Arct. Alp. Res.* **1997**, *29*, 367–378.

44. Auerbach, N.A.; Walker, D.A.; Bockheim, J.G. *Land Cover Map of the Kuparuk River Basin, Alaska*; Institute of Arctic and Alpine Research, University of Colorado: Boulder, CO, USA, 1997.
45. Walker, D.A.; Daniëls, F.J.A.; Alsos, I.; Bhatt, U.S.; Breen, A.L.; Buchhorn, M.; Bültmann, H.; Druckenmiller, L.A.; Edwards, M.E.; Ehrich, D.; et al. Circumpolar Arctic vegetation: A hierarchic review and roadmap toward an internationally consistent approach to survey, archive and classify tundra plot data. *Environ. Res. Lett.* **2016**, *11*, 055005.
46. Muller, S.; Racoviteanu, A.; Walker, D. Landsat MSS-derived land-cover map of northern Alaska: Extrapolation methods and a comparison with photo-interpreted and AVHRR-derived maps. *Int. J. Remote Sens.* **1999**, *20*, 2921–2946.
47. Zubrzycki, S.; Kutzbach, L.; Grosse, G.; Desyatkin, A.; Pfeiffer, E.M. Organic carbon and total nitrogen stocks in soils of the Lena River Delta. *Biogeosciences* **2013**, *10*, 3507–3524.
48. Terentieva, I.E.; Glagolev, M.V.; Lapshina, E.D.; Sabrekov, A.F.; Maksyutov, S. Mapping of West Siberian taiga wetland complexes using Landsat imagery: Implications for methane emissions. *Biogeosciences* **2016**, *13*, 4615–4626.
49. Heikkinen, J.; Virtanen, T.; Huttunen, J.; Elsakov, V.; Martikainen, P. Carbon balance in East European tundra. *Glob. Biogeochem. Cycles* **2004**, *18*, doi:10.1029/2003GB002054.
50. Kuhry, P.; Mazhitova, G.G.; Forest, P.A.; Deneva, S.; Virtanen, T.; Kultti, S. Upscaling soil organic carbon estimates for the Usa Basin (Northeast European Russia) using GIS-based land cover and soil classification schemes. *Geogr. Tidsskr.-Dan. J. Geogr.* **2002**, *102*, 11–25.
51. Marushchak, M.E.; Kiepe, I.; Biasi, C.; Elsakov, V.; Friberg, T.; Johansson, T.; Soegaard, H.; Virtanen, T.; Martikainen, P.J. Carbon dioxide balance of subarctic tundra from plot to regional scales. *Biogeosciences* **2013**, *10*, 437–452.
52. Hugelius, G. Spatial upscaling using thematic maps: An analysis of uncertainties in permafrost soil carbon estimates. *Glob. Biogeochem. Cycles* **2012**, *26*, doi:10.1029/2011GB004154.
53. Jorgensen, C.J.; Johansen, K.M.L.; Westergaard-Nielsen, A.; Elberling, B. Net regional methane sink in High Arctic soils of northeast Greenland. *Nat. Geosci.* **2015**, *8*, 20–23.
54. Elberling, B.; Tamstorf, M.P.; Michelsen, A.; Arndal, M.F.; Sigsgaard, C.; Illeris, L.; Bay, C.; Hansen, B.U.; Christensen, T.R.; Hansen, E.S.; et al. Soil and plant community-characteristics and dynamics at Zackenberg. In *High-Arctic Ecosystem Dynamics in a Changing Climate*; Advances in Ecological Research; Academic Press: New York, NY, USA, 2008; Volume 40, pp. 223–248.
55. Palmtag, J.; Hugelius, G.; Lashchinskiy, N.; Tamstorf, M.P.; Richter, A.; Elberling, B.; Kuhry, P. Storage, landscape distribution, and burial history of soil organic matter in contrasting areas of continuous permafrost. *Arct. Antarct. Alp. Res.* **2015**, *47*, 71–88.
56. Siewert, M.B.; Hanisch, J.; Weiss, N.; Kuhry, P.; Maximov, T.C.; Hugelius, G. Comparing carbon storage of Siberian tundra and taiga permafrost ecosystems at very high spatial resolution. *J. Geophys. Res. Biogeosci.* **2015**, *120*, 1973–1994.
57. Johansen, B.E.; Karlsen, S.R.; Tømmervik, H. Vegetation mapping of Svalbard utilising Landsat TM/ETM+ data. *Polar Rec.* **2012**, *48*, 47–63.
58. Johansen, B.; Tømmervik, H. The relationship between phytomass, NDVI and vegetation communities on Svalbard. *Int. J. Appl. Earth Obs. Geoinf.* **2014**, *27*, 20–30.
59. Hartley, I.P.; Hill, T.C.; Wade, T.J.; Clement, R.J.; Moncrieff, J.B.; Prieto-Blanco, A.; Disney, M.I.; Huntley, B.; Williams, M.; Howden, N.J.K.; et al. Quantifying landscape-level methane fluxes in subarctic Finland using a multiscale approach. *Glob. Chang. Biol.* **2015**, *21*, 3712–3725.
60. Morgenstern, A.; Grosse, G.; Guenther, F.; Fedorova, I.; Schirrmeister, L. Spatial analyses of thermokarst lakes and basins in Yedoma landscapes of the Lena Delta. *Cryosphere* **2011**, *5*, 849–867.
61. Bartsch, A.; Gude, M.; Jonasson, C.; Scherer, D. Identification of geomorphic process units in Karkevagge, northern Sweden, by remote sensing and digital terrain analysis. *Geogr. Ann. Ser. A-Phys. Geogr.* **2002**, *84A*, 171–178.
62. Bartsch, A.; Gude, M.; Gurney, S.D. A geomatics-based approach for the derivation of the spatial distribution of sediment transport processes in periglacial mountain environments. *Earth Surf. Proc. Landf.* **2008**, *33*, 2255–2265.

63. Liljedahl, A.K.; Boike, J.; Daanen, R.P.; Fedorov, A.N.; Frost, G.V.; Grosse, G.; Hinzman, L.D.; Iijma, Y.; Jorgenson, J.C.; Matveyeva, N.; et al. Pan-Arctic ice-wedge degradation in warming permafrost and its influence on tundra hydrology. *Nat. Geosci.* **2016**, *9*, 312–318.
64. Grosse, G.; Schirrmeister, L.; Malthus, T. Application of Landsat-7 satellite data and a DEM for the quantification of thermokarst-affected terrain types in the periglacial Lena-Anabar coastal lowland. *Polar Res.* **2006**, *25*, 51–67.
65. Ulrich, M.; Grosse, G.; Chabrilat, S.; Schirrmeister, L. Spectral characterization of periglacial surfaces and geomorphological units in the Arctic Lena Delta using field spectrometry and remote sensing. *Remote Sens. Environ.* **2009**, *113*, 1220–1235.
66. Turner, K.W.; Wolfe, B.B.; Edwards, T.W.D.; Lantz, T.C.; Hall, R.I.; Larocque, G. Controls on water balance of shallow thermokarst lakes and their relations with catchment characteristics: A multi-year, landscape-scale assessment based on water isotope tracers and remote sensing in Old Crow Flats, Yukon (Canada). *Glob. Chang. Biol.* **2014**, *20*, 1585–1603.
67. Heindel, R.C.; Chipman, J.W.; Virginia, R.A. The Spatial Distribution and Ecological Impacts of Aeolian Soil Erosion in Kangerlussuaq, West Greenland. *Ann. Assoc. Am. Geogr.* **2015**, *105*, 875–890.
68. Leibman, M.O.; Khomutov, A.; Gubarkov, A.; Mullanurov, D.; Dvornikov, Y. The research station Vaskiny Dachi, Central Yamal, West Siberia, Russia—A review of 25 years of permafrost studies. *Fenn. Int. J. Geogr.* **2015**, *153*, 330.
69. Beck, I.; Ludwig, R.; Bernier, M.; Levesque, E.; Boike, J. Assessing Permafrost Degradation and Land Cover Changes (1986–2009) using Remote Sensing Data over Umiujaq, Sub-Arctic Quebec. *Permafr. Periglac. Proc.* **2015**, *26*, 129–141.
70. Muster, S.; Heim, B.; Abnizova, A.; Boike, J. Water body distributions across scales: A remote sensing based comparison of three Arctic tundra wetlands. *Remote Sens.* **2013**, *5*, 1498–1523.
71. Widhalm, B.; Bartsch, A.; Leibman, M.; Khomutov, A. Active layer thickness estimation from X-band SAR backscatter intensity. *Cryosphere Discuss.* **2016**, *2016*, 1–18.
72. Ou, C.; Leblon, B.; Zhang, Y.; LaRocque, A.; Webster, K.; McLaughlin, J. Modelling and mapping permafrost at high spatial resolution using Landsat and Radarsat images in northern Ontario, Canada: Part 1—Model calibration. *Int. J. Remote Sens.* **2016**, *37*, 2727–2750.
73. Ou, C.; LaRocque, A.; Leblon, B.; Zhang, Y.; Webster, K.; McLaughlin, J. Modelling and mapping permafrost at high spatial resolution using Landsat and Radarsat-2 images in Northern Ontario, Canada: Part 2—Regional mapping. *Int. J. Remote Sens.* **2016**, *37*, 2751–2779.
74. Jorgenson, M.T.; Roth, J.E.; Miller, P.F.; Macander, M.J.; Duffy, M.S.; Pullman, E.R.; Miller, E.A.; Attanas, L.B.; Wells, A.F.; Talbot, S. An ecological land survey and landcover map of the Selawik National Wildlife Refuge. Technical Report; ABR, Inc.—Environmental Research & Services and U.S. Fish and Wildlife Service: Kotzebue, AK, USA, 2009.
75. Cable, W.L.; Romanovsky, V.E.; Jorgenson, M.T. Scaling-up permafrost thermal measurements in western Alaska using an ecotype approach. *Cryosphere* **2016**, *10*, 2517–2532.
76. Bartsch, A.; Widhalm, B.; Kuhry, P.; Hugelius, G.; Palmtag, J.; Siewert, M. Can C-Band SAR be used to estimate soil organic carbon storage in tundra? *Biogeosci. Discuss.* **2016**, *2016*, 1–24.
77. Reschke, J.; Bartsch, A.; Schlaffer, S.; Schepaschenko, D. Capability of C-band SAR for operational wetland monitoring at high latitudes. *Remote Sens.* **2012**, *4*, 2923–2943.
78. Bartsch, A.; Wagner, W.; Scipal, K.; Pathe, C.; Sabel, D.; Wolski, P. Global monitoring of wetlands—The value of ENVISAT ASAR Global mode. *J. Environ. Manag.* **2009**, *90*, 2226–2233.
79. Widhalm, B.; Bartsch, A.; Heim, B. A novel approach for the characterization of tundra wetland regions with C-band SAR satellite data. *Int. J. Remote Sens.* **2015**, *36*, 5537–5556.
80. Selkowitz, D.J. A comparison of multi-spectral, multi-angular, and multi-temporal remote sensing datasets for fractional shrub canopy mapping in Arctic Alaska. *Remote Sens. Environ.* **2010**, *114*, 1338–1352.
81. Smith, L.C.; Sheng, Y.; MacDonald, G.M.; Hinzman, L.D. Disappearing Arctic lakes. *Science* **2005**, *308*, 1429–1429.
82. Kumpula, T.; Pajunen, A.; Kaarlejarvi, E.; Forbes, B.C.; Stammner, F. Land use and land cover change in Arctic Russia: Ecological and social implications of industrial development. *Glob. Environ. Chang.-Hum. Policy Dimens.* **2011**, *21*, 550–562.

83. Stow, D.; Hope, A.; McGuire, D.; Verbyla, D.; Gamon, J.; Huemmrich, F.; Houston, S.; Racine, C.; Sturm, M.; Tape, K.; et al. Remote sensing of vegetation and land-cover change in Arctic Tundra Ecosystems. *Remote Sens. Environ.* **2004**, *89*, 281–308.
84. Bhatt, U.S.; Walker, D.A.; Reynolds, M.K.; Bieniek, P.A.; Epstein, H.E.; Comiso, J.C.; Pinzon, J.E.; Tucker, C.J.; Polyakov, I.V. Recent declines in warming and vegetation greening trends over pan-Arctic tundra. *Remote Sens.* **2013**, *5*, 4229–4254.
85. Urban, M.; Forkel, M.; Eberle, J.; Huettich, C.; Schmullius, C.; Herold, M. Pan-Arctic climate and land cover trends derived from multi-variate and multi-scale analyses (1981–2012). *Remote Sens.* **2014**, *6*, 2296–2316.
86. Fraser, R.H.; Olthof, I.; Carriere, M.; Deschamps, A.; Pouliot, D. Detecting long-term changes to vegetation in northern Canada using the Landsat satellite image archive. *Environ. Res. Lett.* **2011**, *6*, 045502.
87. Frost, G.V.; Epstein, H.E.; Walker, D.A. Regional and landscape-scale variability of Landsat-observed vegetation dynamics in northwest Siberian tundra. *Environ. Res. Lett.* **2014**, *9*, doi:10.1088/1748-9326/9/2/025004.
88. Fraser, R.; Olthof, I.; Carriere, M.; Deschamps, A.; Pouliot, D. A method for trend-based change analysis in Arctic tundra using the 25-year Landsat archive. *Polar Rec.* **2012**, *48*, 83–93.
89. Nitze, I.; Grosse, G. Detection of landscape dynamics in the Arctic Lena Delta with temporally dense Landsat time-series stacks. *Remote Sens. Environ.* **2016**, *181*, 27–41.
90. Reynolds, M.K.; Walker, D.A. Increased wetness confounds Landsat-derived NDVI trends in the central Alaska North Slope region, 1985–2011. *Environ. Res. Lett.* **2016**, *11*, doi:10.1088/1748-9326/11/8/085004.
91. Donchyts, G.; Baart, F.; Winsemius, H.; Gorelick, N.; Kwadijk, J.; van de Giesen, N. Earth's surface water change over the past 30 years. *Nat. Clim. Chang.* **2016**, *6*, 810–813.
92. Lin, D.H.; Johnson, D.R.; Andresen, C.; Tweedie, C.E. High spatial resolution decade-time scale land cover change at multiple locations in the Beringian Arctic (1948–2000s). *Environ. Res. Lett.* **2012**, *7*, 025502.
93. Silapaswan, C.; Verbyla, D.; McGuire, A. Land cover change on the Seward Peninsula: The use of remote sensing to evaluate the potential influences of climate warming on historical vegetation dynamics. *Can. J. Remote Sens.* **2001**, *27*, 542–554.
94. Rees, W.; Williams, M. Monitoring changes in land cover induced by atmospheric pollution in the Kola Peninsula, Russia, using Landsat-MSS data. *Int. J. Remote Sens.* **1997**, *18*, 1703–1723.
95. Tommervik, H.; Hogda, K.A.; Solheim, L. Monitoring vegetation changes in Pasvik (Norway) and Pechenga in Kola Peninsula (Russia) using multitemporal Landsat MSS/TM data. *Remote Sens. Environ.* **2003**, *85*, 370–388.
96. Ranson, K.; Sun, G.; Kharuk, V.; Kovacs, K. Assessing tundra-taiga boundary with multi-sensor satellite data. *Remote Sens. Environ.* **2004**, *93*, 283–295.
97. Hufkens, K.; Scheunders, P.; Ceulemans, R. Validation of the sigmoid wave curve fitting algorithm on a forest-tundra ecotone in the Northwest Territories, Canada. *Ecol. Inf.* **2009**, *4*, 1–7.
98. Montesano, P.M.; Neigh, C.S.R.; Sexton, J.; Feng, M.; Channan, S.; Ranson, K.J.; Townshend, J.R. Calibration and Validation of Landsat Tree Cover in the Taiga-Tundra Ecotone. *Remote Sens.* **2016**, *8*, 551.
99. Beck, P.S.A.; Horning, N.; Goetz, S.J.; Loranty, M.M.; Tape, K.D. Shrub Cover on the North Slope of Alaska: A circa 2000 Baseline Map. *Arct. Antarct. Alp. Res.* **2011**, *43*, 355–363.
100. Bartsch, A.; Kumpula, J.; Colpaert, A. Applicability of Remote Sensing to small scale vegetation and reindeer pasture inventory—A study from northern Finland. *Nord. Geogr. Publ.* **1999**, *28*, 103–113.
101. Rees, W.; Williams, M.; Vitebsky, P. Mapping land cover change in a reindeer herding area of the Russian Arctic using Landsat TM and ETM+ imagery and indigenous knowledge. *Remote Sens. Environ.* **2003**, *85*, 441–452.
102. Tommervik, H.; Johansen, B.; Tombre, I.; Thannheiser, D.; Hogda, K.; Gaare, E.; Wielgolaski, F. Vegetation changes in the Nordic mountain birch forest: The influence of grazing and climate change. *Arct. Antarct. Alp. Res.* **2004**, *36*, 323–332.
103. Nordberg, M.; Allard, A. A remote sensing methodology for monitoring lichen cover. *Can. J. Remote Sens.* **2002**, *28*, 262–274.
104. Cihlar, J.; Guindon, B.; Beaubien, J.; Latifovic, R.; Peddle, D.; Wulder, M.; Fernandes, R.; Kerr, J. From need to product: A methodology for completing a land cover map of Canada with Landsat data. *Can. J. Remote Sens.* **2003**, *29*, 171–186.
105. Olthof, I.; Butson, C.; Fernandes, R.; Fraser, R.; Latifovic, R.; Oraziotti, J. Landsat ETM plus mosaic of northern Canada. *Can. J. Remote Sens.* **2005**, *31*, 412–419.

106. Selkowitz, D.J.; Stehman, S.V. Thematic accuracy of the National Land Cover Database (NLCD) 2001 land cover for Alaska. *Remote Sens. Environ.* **2011**, *115*, 1401–1407.
107. Gould, W.; Edlund, S.; Zoltai, S.; Reynolds, M.; Walker, D.; Maier, H. Canadian Arctic vegetation mapping. *Int. J. Remote Sens.* **2002**, *23*, 4597–4609.
108. Gould, W.; Reynolds, M.; Walker, D. Vegetation, plant biomass, and net primary productivity patterns in the Canadian Arctic. *J. Geophys. Res.-Atmos.* **2003**, *108*, doi:10.1029/2001JD000948.
109. Walker, D.; Reynolds, M.; Daniels, F.; Einarsson, E.; Elvebakk, A.; Gould, W.; Katenin, A.; Kholod, S.; Markon, C.; Melnikov, E.; et al. The Circumpolar Arctic vegetation map. *J. Veg. Sci.* **2005**, *16*, 267–282.
110. Rees, W.G.; Danks, F.S. Derivation and assessment of vegetation maps for reindeer pasture analysis in Arctic European Russia. *Polar Rec.* **2007**, *43*, 290–304.
111. Bartalev, S.; Belward, A.; Erchov, D.; Isaev, A. A new SPOT4-VEGETATION derived land cover map of Northern Eurasia. *Int. J. Remote Sens.* **2003**, *24*, 1977–1982.
112. Sulla-Menashe, D.; Friedl, M.A.; Krankina, O.N.; Baccini, A.; Woodcock, C.E.; Sibley, A.; Sun, G.; Kharuk, V.; Elsakov, V. Hierarchical mapping of Northern Eurasian land cover using MODIS data. *Remote Sens. Environ.* **2011**, *115*, 392–403.
113. De Grandi, G.; Spirolazzi, V.; Rauste, Y.; Curto, L.; Rosenqvist, A.; Shimada, M. The GBFM radar mosaic of the Eurasian Taiga: Selected topics on Geo-location and preliminary thematic products. In Proceedings of the IGARSS 2004: IEEE International Geoscience and Remote Sensing Symposium, Anchorage, AK, USA, 20–24 September 2004; pp. 507–510.
114. Whitcomb, J.; Moghaddam, M.; McDonald, K.; Kellendorfer, J.; Podest, E. Mapping vegetated wetlands of Alaska using L-band radar satellite imagery. *Can. J. Remote Sens.* **2009**, *35*, 54–72.
115. Melentyev, V.V.; Matelenok, I.V. Technique for latitudinal discrimination of Siberian landscapes based on satellite passive microwave data. *Contemp. Probl. Ecol.* **2014**, *7*, 827–837.
116. Blunden, J.; Arndt, D.S. State of the Climate in 2015. *Bull. Am. Meteorol. Soc.* **2016**, *97*, SI-S275, doi:10.1175/2016BAMSStateoftheClimate.1.
117. Loveland, T.; Reed, B.; Brown, J.; Ohlen, D.; Zhu, Z.; Yang, L.; Merchant, J. Development of a global land cover characteristics database and IGBP DISCover from 1 km AVHRR data. *Int. J. Remote Sens.* **2000**, *21*, 1303–1330.
118. Hansen, M.; Defries, R.; Townshend, J.; Sohlberg, R. Global land cover classification at 1 km spatial resolution using a classification tree approach. *Int. J. Remote Sens.* **2000**, *21*, 1331–1364.
119. Friedl, M.; McIver, D.; Hodges, J.; Zhang, X.; Muchoney, D.; Strahler, A.; Woodcock, C.; Gopal, S.; Schneider, A.; Cooper, A.; et al. Global land cover mapping from MODIS: Algorithms and early results. *Remote Sens. Environ.* **2002**, *83*, 287–302.
120. Friedl, M.A.; Sulla-Menashe, D.; Tan, B.; Schneider, A.; Ramankutty, N.; Sibley, A.; Huang, X. MODIS Collection 5 global land cover: Algorithm refinements and characterization of new datasets. *Remote Sens. Environ.* **2010**, *114*, 168–182.
121. Bartholome, E.; Belward, A. GLC2000: A new approach to global land cover mapping from Earth observation data. *Int. J. Remote Sens.* **2005**, *26*, 1959–1977.
122. Arino, O.; Bontemps, S.; Defourny, P.; Kalogirou, V.; Ramos Perez, J.J.; Van Bogaert, E.; Weber, J.L. *Pan-European Land Cover/Use Map for 2009*; Pangaea: Bremerhaven, Germany, 2010.
123. Arino, O.; Bicheron, P.; Achard, F.; Latham, J.; Witt, R.; Weber, J.L. GLOBCOVER The most detailed portrait of Earth. *Esa Bull.-Eur. Space Agency* **2008**, *136*, 24–31.
124. Chen, J.; Chen, J.; Liao, A.; Cao, X.; Chen, L.; Chen, X.; He, C.; Han, G.; Peng, S.; Lu, M.; et al. Global land cover mapping at 30 m resolution: A POK-based operational approach. *ISPRS J. Photogramm. Remote Sens.* **2015**, *103*, 7–27.
125. Masson, V.; Champeaux, J.; Chauvin, F.; Meriguet, C.; Lacaze, R. A global database of land surface parameters at 1-km resolution in meteorological and climate models. *J. Clim.* **2003**, *16*, 1261–1282.
126. Champeaux, J.; Masson, V.; Chauvin, R. ECOCLIMAP: A global database of land surface parameters at 1 km resolution. *Meteorol. Appl.* **2005**, *12*, 29–32.
127. Frey, K.E.; Smith, L.C. How well do we know northern land cover? Comparison of four global vegetation and wetland products with a new ground-truth database for West Siberia. *Glob. Biogeochem. Cycles* **2007**, *21*, doi:10.1029/2006GB002706.

128. Du, J.; Kimball, J.; Jones, L.; Watts, J. Implementation of satellite based fractional water cover indices in the pan-Arctic region using AMSR-E and MODIS. *Remote Sens. Environ.* **2016**, *184*, 469–481.
129. Pflugmacher, D.; Krankina, O.N.; Cohen, W.B.; Friedl, M.A.; Sulla-Menashe, D.; Kennedy, R.E.; Nelson, P.; Loboda, T.V.; Kuemmerle, T.; Dyukarev, E.; et al. Comparison and assessment of coarse resolution land cover maps for Northern Eurasia. *Remote Sens. Environ.* **2011**, *115*, 3539–3553.
130. McCallum, I.; Obersteiner, M.; Nilsson, S.; Shvidenko, A. A spatial comparison of four satellite derived 1 km global land cover datasets. *Int. J. Appl. Earth Obs. Geoinf.* **2006**, *8*, 246–255.
131. Porada, P.; Ekici, A.; Beer, C. Effects of bryophyte and lichen cover on permafrost soil temperature at large scale. *Cryosphere Discuss.* **2016**, *2016*, 1–31.
132. Mayaux, P.; Eva, H.; Gallego, J.; Strahler, A.H.; Herold, M.; Agrawal, S.; Naumov, S.; De Miranda, E.E.; Di Bella, C.M.; Ordoyne, C.; et al. Validation of the global land cover 2000 map. *IEEE Trans. Geosci. Remote Sens.* **2006**, *44*, 1728–1739.
133. Bontemps, S.; Boettcher, M.; Brockmann, C.; Kirches, G.; Lamarche, C.; Radoux, J.; Santoro, M.; Vanbogaert, E.; Wegmüller, U.; Herold, M.; et al. Multi-year global land cover mapping at 300 m and characterization for climate modeling: Achievements of the Land Cover component of the ESA Climate Change Initiative. *ISPRS Int. Arch. Photogramm. Remote Sens. Spat. Inf. Sci.* **2015**, *XL-7/W3*, 323–328.
134. Loveland, T.; Belward, A. The IGBP-DIS global 1 km land cover data set, DISCover: First results. *Int. J. Remote Sens.* **1997**, *18*, 3291–3295.
135. CCI LC Project. *CCI-LC Product User Guide*; Technical Report; UCL-Geomatics: Louvain-la-Neuve, Belgium, 2016.
136. CAVM Team. *Circumpolar Arctic Vegetation Map. Scale 1:7,500,000*; Map 1, Conservation of Arctic Flora and Fauna (CAFF); U.S. Fish and Wildlife Service: Anchorage, AK, USA, 2003.
137. Wullschleger, S.D.; Epstein, H.E.; Box, E.O.; Euskirchen, E.S.; Goswami, S.; Iversen, C.M.; Kattge, J.; Norby, R.J.; van Bodegom, P.M.; Xu, X. Plant functional types in Earth system models: Past experiences and future directions for application of dynamic vegetation models in high-latitude ecosystems. *Ann. Bot.* **2014**, *114*, 1–16.
138. Langford, Z.; Kumar, J.; Hoffman, F.M.; Norby, R.J.; Wullschleger, S.D.; Sloan, V.L.; Iversen, C.M. Mapping Arctic Plant Functional Type Distributions in the Barrow Environmental Observatory Using WorldView-2 and LiDAR Datasets. *Remote Sens.* **2016**, *8*, 733.
139. Santoro, M.; Wegmueller, U. Multi-temporal synthetic aperture radar metrics applied to map open water bodies. *IEEE J. Sel. Top. Appl. Earth Obs. Remote Sens.* **2014**, *7*, 3225–3238.
140. Santoro, M.; Beer, C.; Cartus, O.; Schmullius, C.; Shvidenko, A.; McCallum, I.; Wegmüller, U.; Wiesmann, A. Retrieval of growing stock volume in boreal forest using hyper-temporal series of Envisat ASAR ScanSAR backscatter measurements. *Remote Sens. Environ.* **2011**, *115*, 490–507.
141. Duguay, Y.; Bernier, M.; Levesque, E.; Tremblay, B. Potential of C and X band SAR for shrub growth monitoring in sub-Arctic environments. *Remote Sens.* **2015**, *7*, 9410–9430.
142. Fraser, R.H.; Olthof, I.; Lantz, T.C.; Schmitt, C. UAV photogrammetry for mapping vegetation in the low-Arctic. *Arct. Sci.* **2016**, *2*, 79–102.
143. Mora, C.; Vieira, G.; Pina, P.; Lousada, M.; Christiansen, H.H. Land cover classification using high-resolution aerial photography in Adventdalen, Svalbard. *Geogr. Ann. Ser. A Phys. Geogr.* **2015**, *97*, 473–488.
144. Tommervik, H.; Karlsen, S.R.; Nilsen, L.; Johansen, B.; Storvold, R.; Zmarz, A.; Beck, P.S.; Hogda, K.A.; Goetz, S.; Park, T.; et al. Use of unmanned aircraft systems (UAS) in a multi-scale vegetation index study of arctic plant communities in Adventdalen on Svalbard. In Proceedings of the EARSeL eProceedings, Special Issue: 34th EARSeL Symposium, European Association of Remote Sensing Laboratories, Warsaw, Poland, 16–20 June 2014; pp. 47–52.
145. Schneider, J.; Grosse, G.; Wagner, D. *The Lena River Delta—Land Cover Classification of Tundra Environments Based on Landsat 7 ETM+ Data and Its Application for Upscaling of Methane Emissions*; Pangaea: Bremerhaven, Germany, 2009.

